

Goodwin Accelerator Model Revisited with Piecewise Linear Delay Investment

Akio Matsumoto¹, Keiko Nakayama², Ferenc Szidarovszky³

¹Department of Economics, International Center for Further Development of Dynamic Economic Research, Chuo University, Hachioji, Japan

²Department of Economics, Chukyo University, Nagoya, Japan

³Department of Applied Mathematics, University of Pécs, Pécs, Hungary

Email: akiom@tamacc.chuo-u.ac.jp, nakayama@mecl.chukyo-u.ac.jp, szidarka@gmail.com

How to cite this paper: Matsumoto, A., Nakayama, K. and Szidarovszky, F. (2018) Goodwin Accelerator Model Revisited with Piecewise Linear Delay Investment. *Advances in Pure Mathematics*, 8, 178-217. <https://doi.org/10.4236/apm.2018.82010>

Received: January 24, 2018

Accepted: February 25, 2018

Published: February 28, 2018

Copyright © 2018 by authors and Scientific Research Publishing Inc.

This work is licensed under the Creative Commons Attribution International License (CC BY 4.0).

<http://creativecommons.org/licenses/by/4.0/>



Open Access

Abstract

It is well-known that Goodwin's nonlinear delay accelerator model can generate diverse oscillations (*i.e.*, smooth and sawtooth oscillations). It is, however, less-known what conditions are needed for these dynamics to emerge. In this study, using a piecewise linear investment function, we solve the governing delay differential equation and obtain the explicit forms of the time trajectories. In doing so, we detect conditions for persistent oscillations and also conditions for the birth of such cyclic dynamics.

Keywords

Nonlinear Accelerator, Investment Delay, Successive Integration, Smooth and Kinked Solutions, Numerical Analysis

1. Introduction

It has been well-known that Goodwin's business cycle model with a delayed nonlinear accelerator [1] can generate multiple solutions. Depending on specified forms of the initial functions and specified parameter values, it gives rise to smooth cyclic oscillations or sawtooth (*i.e.*, slow-rapid) oscillations. This paper aims to analytically and numerically investigate these cyclic properties of Goodwin's model by solving the time delay equations and performing simulations.

[1] presents five different versions of the nonlinear accelerator-multiplier model with investment delay. The first version has the simplest form assuming a piecewise linear function with three levels of investment and aims to exhibit how non-linearities give rise to endogenous cycles without relying on structurally un-

stable parameters, exogenous shocks, etc. The second version replaces the piecewise linear investment function with a smooth nonlinear investment function. Although persistent cyclical oscillations are shown to exist, the second version includes unfavorable phenomena, that is, discontinuous investment jumps, which are not observed in the real economic world. “In order to come close to reality” ([1], p. 11), the third version introduces an investment delay. However, no analytical considerations are given to this version. The existence of an endogenous business cycle is confirmed in the fourth version, which is a linear approximation of the third version with respect to the investment delay. Finally, alternation of autonomous expenditure over time is taken into account in the fifth version, which becomes a forced oscillation system.

This paper reconstructs the third version having a piecewise linear investment function with fixed time delay. It is a complement to [2] in which the effects caused by investment delay as well as consumption delay are considered. It is also an extension of [3] in which the dynamics of Goodwin’s model is examined under continuously distributed time delays and the existence of the multiple limit cycles is analytically and numerically shown. Following the method of successive integration provided by [4], we derive explicit forms of the solutions and obtain conditions under which the smooth or sawtooth oscillations emerge. With the same spirit, [5] examines Goodwin’s model. Their focus is mainly put on the relaxation (*i.e.*, sawtooth) oscillations. We step forward and investigate periodic properties of the smooth oscillations, which will be called Goodwin oscillations henceforth. Our main concerns in this paper are on the role of the fixed delay for the birth of cyclic macro dynamics

The paper is organized as follows. In Section 2, the Goodwin model without delay is considered to see how nonlinearities of the model contribute emergence of cyclic dynamics. In Section 3, an investment delay is introduced to construct. Effects of investment delay on the smooth oscillations are considered in Section 4 and those on the sawtooth oscillations are done in Section 5. Section 6 contains some concluding remarks.

2. Basic Model

To find out how nonlinearity works to generate endogenous cycles, we review the second version of Goodwin’s model, which we call the *basic model*,

$$\begin{cases} \varepsilon \dot{y}(t) = \dot{k}(t) - (1 - \alpha)y(t), \\ \dot{k}(t) = \varphi[\dot{y}(t)]. \end{cases} \quad (1)$$

Here k is the capital stock, y the national income, α the marginal propensity to consume, which is positive and less than unity, and the reciprocal of ε is a positive adjustment coefficient. Since the dot over variables means time differentiation, $\dot{k}(t)$ and $\dot{y}(t)$ are the rates of change in capital (*i.e.*, investment) and national income. The first equation of (1) defines an adjustment process of the national income in which national income rises or falls according to whether

investment is larger or smaller than savings. The second equation determines the induced investment based on the acceleration principle with which investment depends on the rate of changes in the national income in the following way,

$$\varphi[\dot{y}(t)] = \begin{cases} 3n & \text{if } \dot{y}(t) \in I_U = \left(\frac{3n}{\nu}, \infty\right), \\ \nu \dot{y}(t) & \text{if } \dot{y}(t) \in I_M = \left[-\frac{n}{\nu}, \frac{3n}{\nu}\right], \\ -n & \text{if } \dot{y}(t) \in I_L = \left(-\infty, -\frac{n}{\nu}\right) \end{cases} \quad (2)$$

where $\nu > 0$ and $n > 0$. This function is piecewise linear and has three distinct regions. Accordingly, there are two threshold values of $\dot{y}(t)$ denoted as $3n/\nu$ and $-n/\nu$ and the investment is proportional to the change in the national income in the middle region, I_M , but becomes perfectly inflexible (i.e., inelastic) in the upper region I_U or the lower region I_L . These values are thought to be “ceiling” and “floor” of investment where the ceiling is assumed to be three time higher than the floor as it was the case in Goodwin’s model.

Inserting the second equation of (1) into the first one and moving the terms on the right hand side to the left give an implicit form of the dynamic equation for national income y ,

$$\varepsilon \dot{y}(t) - \varphi(\dot{y}(t)) + (1 - \alpha)y(t) = 0 \quad (3)$$

where the stationary point of the basic model is $y(t) = \dot{y}(t) = 0$ for all t . With Equation (2) it is reduced to either

$$(\varepsilon - \nu)\dot{y}(t) = -(1 - \alpha)y(t) \quad (4)$$

if $\dot{y}(t)$ is in the middle region or

$$\varepsilon \dot{y}(t) = -(1 - \alpha)y(t) + d \quad (5)$$

where $d = 3n$ if $\dot{y}(t)$ is in the upper region and $d = -n$ if in the lower region. Equations (4) and (5) are linear and thus solvable. We see graphically and then analytically how dynamics proceeds.

2.1. Phase Plot

Solving (4) and (5) for $y(t)$ presents an alternative expression of dynamic equation $\dot{y}(t) = f[\dot{y}(t)]$ where

$$f[\dot{y}(t)] = \begin{cases} \frac{3n - \varepsilon \dot{y}(t)}{1 - \alpha} & \text{if } \dot{y}(t) \in I_U, \\ \frac{(\nu - \varepsilon)\dot{y}(t)}{1 - \alpha} & \text{if } \dot{y}(t) \in I_M, \\ -\frac{n + \varepsilon \dot{y}(t)}{1 - \alpha} & \text{if } \dot{y}(t) \in I_L. \end{cases} \quad (6)$$

Once the initial value is given, the whole evolution of national income is de-

terminated. The phase diagram with $\varepsilon < \nu$ is shown in **Figure 1** in which $y = f(\dot{y})$ is described by a mirror-imaged N -shaped curve in the (\dot{y}, y) plane.¹ The stationary point is at the origin denoted by E . The locus of $y = f(\dot{y})$ is the positive sloping line in the middle region while it is the negative sloping upper or lower line in the upper or lower region. For each value of \dot{y} , there is a unique corresponding y value determined to make a point (\dot{y}, y) satisfy Equation (6) and it is also determined whether y is increasing or decreasing at that point. So the direction of the trajectory is given in all points of the phase diagram. The directions are shown by arrows. Let A denote the local maximum point of the curve with positive y and \dot{y} always, and let C be the local minimum point with negative y and \dot{y} . Point B and D have the same y values as at points A and C , respectively. Notice that the direction of the dynamic evolution goes from $-\infty$ to C , from the origin to C , from the origin to A and also from $+\infty$ to A . Selecting the initial point denoted as S on the positive-sloping line, the evolution starts at this point and moves upward until point A as indicated by arrow. Then it cannot continue on the continuous curve after point A since the direction of evolution changes. Therefore it jumps to point B and continues along the same direction until point C , where the same problem occurs, so another jump occurs to point D and evolution continues until point A , at which the next round repeats itself. Thus the differential Equation (3) with the piecewise linear investment function (2) can give rise to a closed orbit $ABCD$ constituting a self-sustaining slow-rapid oscillation. The stationary point is unstable if $\varepsilon < \nu$, however, the oscillation is stable in a sense that the locus (\dot{y}, y) sooner or later converges to the same oscillation regardless of a

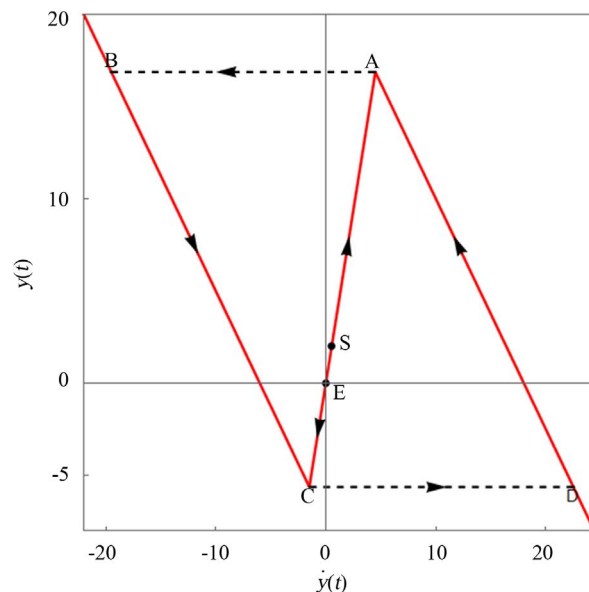


Figure 1. Slow-rapid oscillation along $y = f(\dot{y})$ with $\nu > \varepsilon$.

¹Mathematica version 11 is used to perform simulations and illustrate this and the following figures. The color versions of the figures are found in DP278 at

<http://www.chuo-u.ac.jp/research/institutes/economic/publication/discusion>.

selection of the initial point. This is a simple exhibition of emerging a stable endogenous cycle of national income.

The vertex of the closed oscillation in **Figure 1** are

$$A = \left(\frac{3n}{v}, y_{\max} \right), B = (\dot{y}_m, y_{\max}), C = \left(-\frac{n}{v}, y_{\min} \right) \text{ and } D = (\dot{y}_M, y_{\min})$$

where the maximum and minimum values of \dot{y} along the cycle are

$$\dot{y}_M = \frac{n(4v - \varepsilon)}{\varepsilon v} \text{ and } \dot{y}_m = -\frac{n(4v - 3\varepsilon)}{\varepsilon v}$$

while the maximum and minimum values of y along the cycle are

$$y_{\max} = \frac{3n(v - \varepsilon)}{v(1 - \alpha)} \text{ and } y_{\min} = -\frac{n(v - \varepsilon)}{v(1 - \alpha)}$$

It should be noticed that the instability and the nonlinearity is crucial sources for the birth of persistent oscillations since the instability of the stationary point prevents trajectories from converging and the nonlinearities such as the ceiling and floor prevent trajectories from diverging.

Jumping behavior leads to the kinked time trajectory of $y(t)$ and the discontinuous time trajectory of $\dot{y}(t)$ that are shown as the blue and red curves in **Figure 2**. $A = B$ holds at the upper kinked point of the blue curve and $C = D$ at the lower kinked point. The red trajectory from 0 to t_1 describes the movement of $\dot{y}(t)$ from point S to A . At time t_1 when the left-most red curve defined on interval $[0, t_1]$ arrives at the upper horizontal dotted line, the red curve jumps straightly down to the starting point of the lower red curve defined on interval $[t_1, t_2]$, the point of which correspond to point B . At time t_2 , the red curve crosses the lower dotted line from below and the intersection corresponds to point C at which the red curve jumps straightly

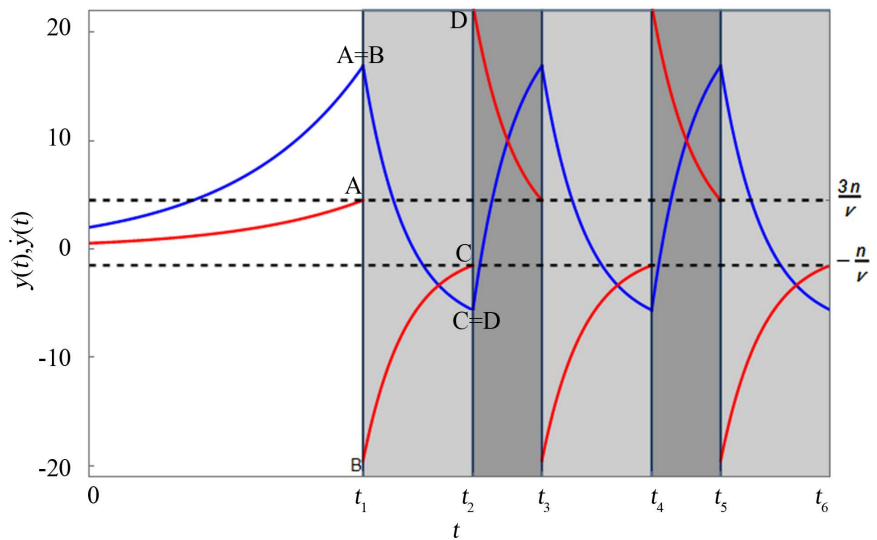


Figure 2. Time trajectories of $y(t)$ (the kinked blue curve) and $\dot{y}(t)$ (the discontinuous red curves).

up to the downward-sloping red curve defined on interval $[t_2, t_3]$, that then crosses the upper horizontal dotted line and the cross-point correspond to point *A*. **Figure 2** illustrates the same dynamics of **Figure 1** from a different view point.

2.2. Explicit Solutions

Selecting an initial point, we can determine an explicit form of the corresponding time trajectory and its rate of change. In particular, we take an initial point on the positive sloping part of the $y(0) = f[\dot{y}(0)]$ curve such as

$$0 < y(0) = \text{constant} \quad \text{and} \quad \dot{y}(0) = \frac{1-\alpha}{\nu-\varepsilon} y(0) < \frac{3n}{\nu}$$

where $y_{\min} < y(0) < y_{\max}$. If $\dot{y}(t)$ is in the middle region, Equation (4) yields explicit forms of the solution $y(t)$ and its time derivative,

$$y_1(t) = e^{\frac{1-\alpha}{\nu-\varepsilon}t} K_1 \quad \text{and} \quad \dot{y}_1(t) = e^{\frac{1-\alpha}{\nu-\varepsilon}t} \left(\frac{1-\alpha}{\nu-\varepsilon} K_1 \right) \quad \text{with} \quad K_1 = y(0) \quad (7)$$

and if $\dot{y}(t)$ enters the upper or lower region, Equation (5) yields the following forms of the solution $y(t)$ and its time derivative,

$$y_i(t) = e^{\frac{1-\alpha}{\varepsilon}t} K_i + \frac{d_i}{1-\alpha} \quad \text{and} \quad \dot{y}_i(t) = e^{\frac{1-\alpha}{\varepsilon}t} \left(-\frac{1-\alpha}{\varepsilon} K_i \right) \quad \text{for} \quad i = 2, 3, \dots \quad (8)$$

where $d_i = -n$ if i is even and $d_i = 3n$ if i is odd.

Since $\dot{y}_1(0) < 3n/\nu$ and $\dot{y}_1(t)$ is increasing in t , solving $\dot{y}_1(t) = 3n/\nu$ for t presents an arrival time $t = t_1$,

$$t_1 = \frac{\nu-\varepsilon}{1-\alpha} \log \left[\frac{3n(\nu-\varepsilon)}{\nu(1-\alpha)K_1} \right].$$

Substituting t_1 into $y_1(t)$ and $\dot{y}_1(t)$ yields

$$y_1(t_1) = y_{\max} \quad \text{and} \quad \dot{y}_1(t_1) = \frac{3n}{\nu}$$

implying that point $(\dot{y}_1(t_1), y_1(t_1))$ corresponds to point *A* in **Figure 1**. Solutions in (7) describe the movement from point *S* to point *A*. At $t = t_1$, the dynamic system (4) is switched to Equation (5) with $d = -n$. Equations in (8) with $i = 2$ presents explicit forms of the solution and its time derivative,

$$y_2(t) = e^{\frac{1-\alpha}{\varepsilon}t} K_2 - \frac{n}{1-\alpha} \quad \text{and} \quad \dot{y}_2(t) = e^{\frac{1-\alpha}{\varepsilon}t} \left(-\frac{1-\alpha}{\varepsilon} K_2 \right). \quad (9)$$

Since the time trajectory $y(t)$ is continuous in t , solving $y_1(t_1) = y_2(t_1)$ gives the value of K_2 ,

$$K_2 = \frac{n(4\nu-\omega)}{\nu(1-\alpha)} e^{\frac{1-\alpha}{\varepsilon}t_1}.$$

With this K_2 , we have

$$\dot{y}_2(t_1) = \dot{y}_m \quad \text{and} \quad y_2(t_1) = y_{\max}.$$

Thus point $(\dot{y}_2(t_1), y_2(t_1))$ corresponds to point B to which point A jumps. This rapid change is described by the vertical movement of the red curve along the vertical line at $t = t_1$ in **Figure 2**. Since $\dot{y}_2(t_1) < -n/v$ and $\dot{y}_2(t)$ increases in t , solving $\dot{y}_2(t) = -n/v$ gives a necessary time to arrive at $-n/v$,

$$t_2 = t_1 + \frac{\omega}{1-\alpha} \log \left[\frac{4v-3\varepsilon}{\varepsilon} \right].$$

In the same way above, it is possible to show that

$$(\dot{y}_2(t_2), y_2(t_2)) = \left(-\frac{n}{v}, y_{\min} \right)$$

which is point C . The movement from point B to C is described by solutions in (9). At time $t = t_2$, the dynamic system with $d = -n$ is switched to the dynamic system with $d = 3n$ and (8) with $i = 3$ presents explicit forms of the solutions

$$y_3(t) = e^{\frac{1-\alpha}{\varepsilon}t} K_3 + \frac{3n}{1-\alpha} \text{ and } \dot{y}_3(t) = e^{\frac{1-\alpha}{\varepsilon}t} \left(-\frac{1-\alpha}{\varepsilon} K_3 \right). \tag{10}$$

Solving $y_2(t_2) = y_3(t_2)$ presents the value of K_3 ,

$$K_3 = -\frac{n(4v-\varepsilon)}{v(1-\alpha)} e^{\frac{1-\alpha}{\varepsilon}t_2}.$$

It is also able to be shown that point $(\dot{y}_3(t_2), y_3(t_2))$ is identical with point D , implying a jump to point D from point C . Solving $\dot{y}_3(t) = 3n/v$ presents a time when $\dot{y}_3(t)$ arrives at $3n/v$,

$$t_3 = t_2 + \frac{\varepsilon}{1-\alpha} \log \left[\frac{4v-\varepsilon}{3\varepsilon} \right].$$

At $t = t_3$, we can confine that the trajectory comes back to point A at which the following holds,

$$(\dot{y}_3(t_3), y_3(t_3)) = \left(\frac{3n}{v}, y_M \right).$$

A new round starts as time goes further and the same procedure is applied to obtain explicit forms of the solutions for $t \geq t_3$. Time segments of $y(t)$ and $\dot{y}(t)$ that constitute one cycle of national income are now given by (9) and (10). Since the length of one cycle is measured by the time period between one upper (or lower) kinked point and next upper (or lower) kinked point, it is given by

$$t_3 - t_1 = \frac{\varepsilon}{1-\alpha} \log \left[\frac{(4v-\varepsilon)(4v-3\varepsilon)}{3\varepsilon^2} \right].$$

Further the length of the recession period along segment BC in which national income is decreasing is

$$t_2 - t_1 = \frac{\omega}{1-\alpha} \log \left[\frac{4v-3\varepsilon}{\varepsilon} \right]$$

while the length of the recovery period along segment DA in which national in-

come is increasing is

$$t_3 - t_2 = \frac{\varepsilon}{1 - \alpha} \log \left[\frac{4\nu - \varepsilon}{3\varepsilon} \right].$$

In what follows, we will perform numerical simulations with the set of the parameter values given below which are the same parameter values used in [1] and [2]. Needless to say, these particular values of the parameters are selected only for analytical simplicity and do not affect qualitative aspects of the results to be obtained.

Assumption 1 $\alpha = 0.6, \varepsilon = 0.5, \theta = 1, \nu = 2$ and $n = 3$

In particular, **Figure 1** and **Figure 2** are illustrated under Assumption 1 and the initial values of $y(0) = 2$ and $\dot{y}(0) = 8/15$, where the pair $(\dot{y}(0), y(0))$ corresponds to point S in **Figure 2**. The critical times at which the system switching occurs are given

$$t_1 \approx 7.998, t_2 \approx 11.204, t_3 \approx 13.216, t_4 \approx 16.422, t_5 \approx 7.998 \text{ and } t_6 \approx 21.640$$

by solving

$$\dot{y}_i(t) = \frac{3n}{\nu} \text{ if } i \text{ is odd or } \dot{y}_i(t) = -\frac{n}{\nu} \text{ if } i \text{ is even.}$$

The length of one cycle given by $t_{i+2} - t_i$ is about 5.218 years.² In the same way, the recession period from one peak to trough of the cycle is given by $t_i - t_{i-1} \approx 3.206$ years for i being even while the recovery period from one trough to peak by $t_i - t_{i-1} \approx 2.012$ years for i being odd. The constant K_i solves

$$y_i(t_i) = y_{i+1}(t_i)$$

with $K_1 = 2$ and the numerical results are as follows,

$$K_2 \approx 14641.52, K_3 \approx -219622.71, K_4 \approx 951698.40, \\ K_5 \approx -14275475.98 \text{ and } K_6 \approx 61860395.91.$$

3. Delay Model

We now investigate how the investment delay affects time paths of national income. Observing the fact that, in real economy, plans and their realizations need time to take effects, [1] introduces the investment delay, $\theta > 0$, between decisions to invest and the corresponding outlays in order, first, to come closer to reality and second, to eliminate unrealistic discontinuous jumps. Consequently the investment function (6) is modified as follows

$$\varphi[\dot{y}(t - \theta)] = \begin{cases} 3n & \text{if } \dot{y}(t - \theta) \text{ in } I_U, \\ \nu \dot{y}(t - \theta) & \text{if } \dot{y}(t - \theta) \text{ in } I_M, \\ -n & \text{if } \dot{y}(t - \theta) \text{ in } I_M. \end{cases} \quad (11)$$

With this modification, the dynamic Equation (3) turns to be

$$\varepsilon \dot{y}(t) - \varphi(\dot{y}(t - \theta)) + (1 - \alpha)y(t) = 0 \quad (12)$$

²In [4], it is assumed that $\theta = 1$ is one year delay. Under the specified values of the parameters, $t_{i+2} - t_i = 5.218$, implying the length is considered to be 5.218 years.

that we call the *delay model*.³ Equation (12) is reduced to a *linear delay differential equation of neutral type* if the delayed rate of change in national income stays in the middle region

$$\varepsilon \dot{y}(t) - v \dot{y}(t - \theta) + (1 - \alpha) y(t) = 0 \quad (13)$$

and it remains to be a linear ordinary differential Equation (5) if the delayed rate is in the upper or lower region. To solve the delay equation, we need an initial function that determines behavior of y prior to time zero,

$$y(t) = \Phi(t) \text{ for } -\theta \leq t \leq 0.$$

Although [1] does not analyze delay dynamics generated by the third version, [4], in addition to numerical analysis, derive the explicit forms of the piecewise continuous solutions of $y(t)$ under the piecewise linear investment function (11). We follow their method of successive integration to solve the delay equation and derive the explicit forms of time trajectories of $y(t)$ and $\dot{y}(t)$. Since a cyclic oscillation has been shown to exist in the basic model, our main concern here is to see how the presence of the investment delay and the selection of the initial function affect characteristics of such a sawtooth oscillation obtained in the basic model.

It has been examined by [4] that the birth of oscillations in the Goodwin model are caused by a selected form of the initial function and the length of delay. For the sake of analytical simplicity, we assume the constant initial function in the following numerical simulations.

$$\textbf{Assumption 2} \quad \Phi(t) = y_0 \neq 0 \text{ and } \dot{\Phi}(t) = 0 \text{ for } -\theta \leq t \leq 0. \quad (14)$$

3.1. Local Stability

It is well known that if the characteristic polynomial of a linear neutral equation has roots only with negative real parts, then the stationary point is locally asymptotically stable. The normal procedure for solving this equation is to try an exponential form of the solution. Substituting $y(t) = y_0 e^{\lambda t}$ into (13) and rearranging terms, we obtain the corresponding characteristic equation:

$$\varepsilon \lambda - v \lambda e^{-\lambda \theta} + (1 - \alpha) = 0.$$

To check stability, we determine conditions under which all roots of this characteristic equation lie in the left or right half of the complex plane. Dividing both sides of the characteristic equation by ε and introducing the new variables

$$a = \frac{v}{\varepsilon} > 0 \text{ and } b = \frac{1 - \alpha}{\varepsilon} > 0, \quad (15)$$

we rewrite the characteristic equation as

$$\lambda - a \lambda e^{-\lambda \theta} + b = 0. \quad (16)$$

[6] derive explicit conditions for stability/instability of the n -th order linear scalar neutral delay differential equation with a single delay. Since (13) is a spe-

³Goodwin assumes a smooth form of the nonlinear investment function in his third version.

cial case of the n -th order equation, applying their result (*i.e.*, Theorem 2.1) leads to the following: the real parts of the solutions of Equation (16) are positive for all $\theta > 0$ if $a > 1$. The first result on the fixed delay model is summarized as follows:

Lemma 1 *If $\nu > \varepsilon$, then the zero solution of the fixed delay model (13) is locally unstable for all $\theta > 0$.*

On the other hand, if $\nu \leq \varepsilon$ or $a \leq 1$, characteristic Equation (16) has at most finitely many eigenvalues with positive real parts. The eigenvalue is real and negative when $\theta = 0$. The roots of the characteristic equation are functions of the delay. Although it is expected that all roots have negative real parts for small values of θ , the real parts of some roots may change their signs to positive from negative as the lengths of the delay increases. The stability of the zero solution may change. Such phenomena are often referred to as *stability switches*. We will next prove that stability switching, however, cannot take place in the delayed model.

Lemma 2 *If $\nu \leq \varepsilon$, then the zero solution of the fixed delay model (13) is locally stable for all $\theta > 0$.*

Proof. 1) It can be checked that $\lambda = 0$ is not a solution of (16) because substituting $\lambda = 0$ yields $b = 0$ that contradicts $b > 0$. If the stability switches at $\theta = \bar{\theta}$, then (16) must have a pair of pure conjugate imaginary roots with $\theta = \bar{\theta}$. Thus to find the critical value of $\bar{\theta}$, we assume that $\lambda = i\omega$, with $\omega > 0$, is a root of (16) for $\theta = \bar{\theta} > 0$. Substituting $\lambda = i\omega$ into (16), we have

$$b - a\omega \sin \omega\theta = 0,$$

and

$$\omega - a\omega \cos \omega\theta = 0.$$

Moving b and ω to the right hand sides and adding the squares of the resultant equations, we obtain

$$b^2 + (1 - a^2)\omega^2 = 0.$$

Since $b > 0$ and $1 - a^2 > 0$ as $a < 1$ is assumed, there is no ω that satisfies the last equation. In other words, there are no roots of (16) crossing the imaginary axis when θ increases. No stability switch occurs and thus the zero solution is locally asymptotically stable for any $\theta > 0$.

2) In case of $\varepsilon = \nu$ in which $a = 1$, the characteristic equation becomes

$$\lambda(1 - e^{-\lambda\theta}) + b = 0. \quad (17)$$

It is clear that $\lambda = 0$ is not a solution of (17) since $b > 0$. Thus we can assume that a root of (17) has non-negative real part, $\lambda = u + iv$ with $u \geq 0$ for some $\theta > 0$. From (17), we have

$$(u + b)^2 + v^2 = e^{-2u\theta}(u^2 + v^2) \leq (u^2 + v^2),$$

where the last inequality is due to $e^{-2u\theta} \leq 1$ for $u \geq 0$ and $\theta > 0$. Hence

$$2ub + b^2 \leq 0,$$

where the direction of inequality contradicts the assumption that $u \geq 0$ and $b > 0$. Hence it is impossible for the characteristic equation to have roots with nonnegative real parts. Accordingly, all roots of (17) must have negative real parts for all $\theta > 0$.

Lemmas 1 and 2 imply the following theorem concerning local stability of the delay model (13).

Theorem 3 For any $\theta > 0$, the zero solution of the delay model (13) is locally asymptotically stable if $\nu \leq \varepsilon$ and unstable if $\nu > \varepsilon$.

We call y_0 in Assumption 2 an initial value for convenience. Fixing the length of delay at $\theta = 1$, we illustrate a bifurcation diagram with respect to the initial value in **Figure 3**. For given value of y_0 , the dynamic system runs for $0 \leq t \leq T = 500$. The solution for $t \leq 450$ are discarded to eliminate the initial disturbances and the maximum and minimum values of the resultant solutions for $450 \leq t \leq 500$ are plotted against y_0 . The bifurcation parameter y_0 increases from -10 to 6 with increment of 0.01 and for each value of y_0 , the same calculation procedure is repeated. As is seen in **Figure 3** and already pointed out by [5], the delay dynamic system with the constant initial function has the two threshold initial values y_0^{\max} and y_0^{\min} such that the sawtooth oscillations arise for $y_0^{\min} \leq y_0 \leq y_0^{\max}$ and so do the Goodwinian oscillations otherwise. These values depend on the length of the delay and are numerically determined as $y_0^{\max} \approx 2.39$ and $y_0^{\min} \approx -6.28$ under $\theta = 1$. In the following, we first set $y_0 = y_0^G = 4.5$ and consider Goodwinian oscillations in Section 4 and then examine sawtooth oscillations with $y_0 = y_0^S = -2$ in Section 5.

4. Goodwinian Oscillations

Given Assumptions 1 and 2 with $y_0 = y_0^G$, the time trajectories of $y(t)$ and $\dot{y}(t)$ are illustrated by the blue and red curves, respectively, in **Figure 4** in

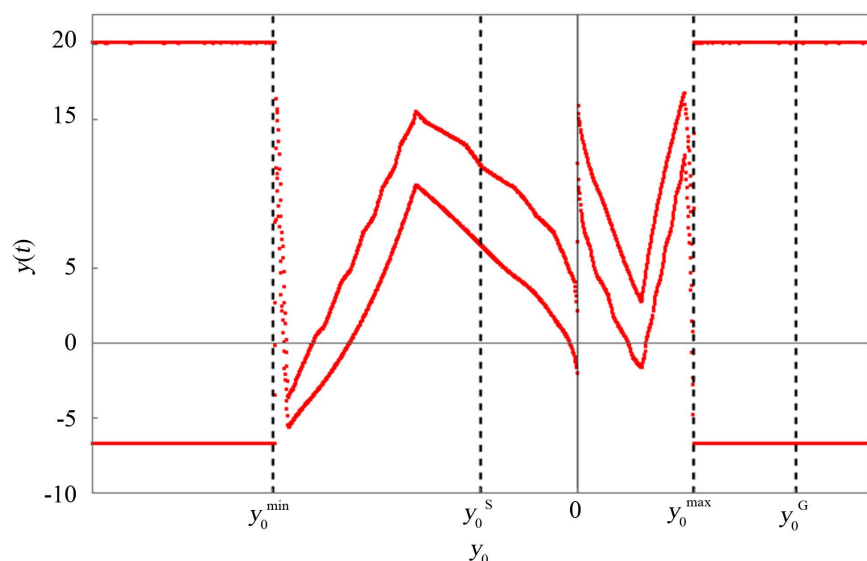


Figure 3. Bifurcation diagram with respect to y_0 .

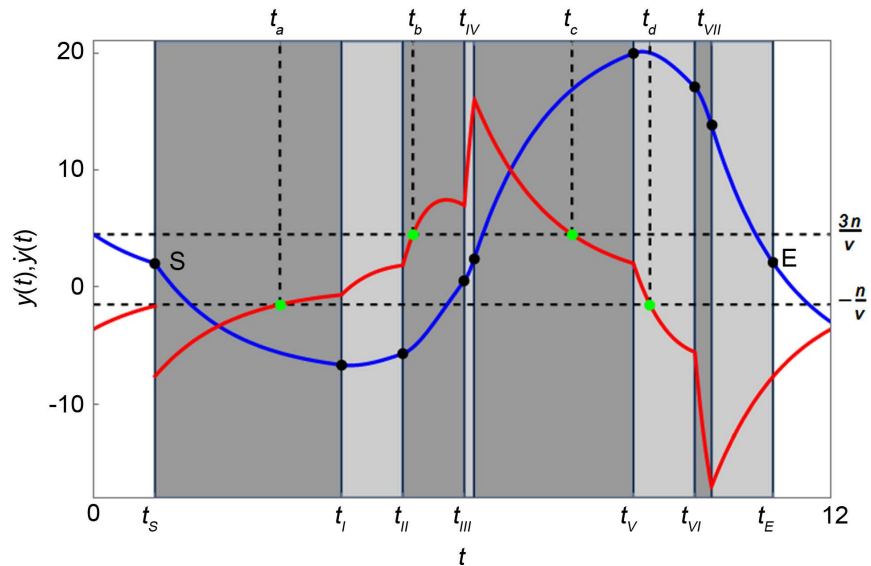


Figure 4. Time trajectories of $y(t)$ and $\dot{y}(t)$.

which we can see that delay time trajectories show sharp differences from non-delay time trajectories depicted in **Figure 2**. The interval including the whole parts of one cycle where $y(t)$ starts at point S and ends at point E is divided into eight subintervals, each of which is distinguished by heavy or light gray color. Solving non-delay dynamic Equation (5) or delay dynamic Equation (13), we will derive the explicit forms of these trajectories in each subinterval where the detailed derivations are presented in Appendix I.

4.1. Time Trajectories

We omit consideration in interval $[0, t_s]$ with $t_s = \theta$ as behavior there strongly depends on a choice of initial point. In the first interval $I_1 = [t_s, t_1]$ where $t_1 = t_a + \theta = 4.03$ and $t_a = 3.03$ solves the equation $\dot{y}_1(t) = -n/v$, the blue and red trajectories are controlled by Equation (5) with $d = -n$,

$$(G-I) \begin{cases} y_1(t) = e^{\frac{1-\alpha}{\varepsilon} t} K_1 - \frac{n}{1-\alpha} \\ \dot{y}_1(t) = e^{\frac{1-\alpha}{\varepsilon} t} \left(-\frac{1-\alpha}{\varepsilon} K_1 \right) \end{cases} \text{ for } t \in I_1$$

where $K_1 \approx 21.19$. At $t = t_a$, the red trajectory $\dot{y}_1(t)$ crosses the lower horizontal dotted line at $-n/v$ and the crossing point is denoted by the left most green dot in **Figure 4**. The boundary values of this interval are

$$y_1(t_s) \approx 2.02, \dot{y}_1(t_s) \approx -7.62 \text{ and } y_1(t_1) \approx -6.66, \dot{y}_1(t_1) \approx 0.67.$$

As seen in **Figure 4**, the blue trajectory is kinked and the red curve jumps downward at $t = t_s$. This discontinuity is shown as follows. Let $y_0(t)$ and $\dot{y}_0(t)$ be a solution and its derivative in interval $[0, t_s]$.⁴ Then, constant K_1 is

⁴The explicit forms are given in Appendix I.

determined so as to satisfy $y_0(t_s) = y_I(t_s)$, that is, the end point of $y_0(t_s)$ is coincided with the starting point of $y_I(t_s)$. Hence it first implies the continuity of $y(t)$ at $t = t_s$. Secondly, the solutions of $y_0(t)$ and $y_I(t)$ should satisfy the following dynamic equations respectively,

$$\begin{aligned} \varepsilon \dot{y}_0(t_s) + (1 - \alpha)y_0(t_s) &= 0, \\ \varepsilon \dot{y}_I(t_s) + (1 - \alpha)y_I(t_s) &= -n. \end{aligned}$$

Subtracting the second equation from the first presents

$$\dot{y}_0(t_s) - \dot{y}_I(t_s) = \frac{n}{\varepsilon} > 0 \text{ or } \dot{y}_0(t_s) > \dot{y}_I(t_s)$$

where the last inequality implies discontinuity of the derivative at $t = t_s$.

In the second interval $I_{II} = [t_I, t_{II}]$ with $t_{II} = t_I + \theta \approx 5.03$, applying successive integration for dynamic equation $\varepsilon \dot{y}(t) + (1 - \alpha)y(t) = v \dot{y}_I(t - \theta)$ gives explicit forms of the solutions,

$$(G-II) \begin{cases} y_{II}(t) = e^{-\frac{1-\alpha}{\varepsilon}t} (\alpha_1^{II}t + \alpha_0^{II}) \\ \dot{y}_{II}(t) = e^{-\frac{1-\alpha}{\varepsilon}t} (\beta_1^{II}t + \beta_0^{II}) \end{cases} \text{ for } t \in I_{II}$$

where

$$\begin{aligned} \alpha_1^{II} &= -\frac{v(1-\alpha)}{\varepsilon^2} e^{-\frac{1-\alpha}{\varepsilon}\theta} K_I \approx -150.92, \\ \beta_1^{II} &= -\frac{1-\alpha}{\varepsilon} \alpha_1^{II} \approx 120.74, \\ \alpha_0^{II} &\approx 440.94, \\ \beta_0^{II} &= \alpha_1^{II} - \frac{1-\alpha}{\varepsilon} \alpha_0^{II} \approx -503.67. \end{aligned}$$

The integral constant α_0^{II} is obtained by solving $y_I(t_I) = y_{II}(t_I)$. The boundary values for the end points of interval I_{II} are

$$y_{II}(t_I) \approx -6.66, \dot{y}_{II}(t_I) \approx 0.67 \text{ and } y_{II}(t_{II}) \approx -5.69, \dot{y}_{II}(t_{II}) \approx 1.85.$$

It can be numerically as well as graphically checked that $y_{II}(t_I) = y_I(t_I)$ and $\dot{y}_{II}(t_I) = \dot{y}_I(t_I)$. In consequence $y_I(t)$ and $y_{II}(t)$ are smoothly connected (*i.e.*, continuous and differentiable). On the other hand, $\dot{y}(t) \geq -n/v$ for $t \geq t_a$ induces system change at $t = t_I$ leading to that $\dot{y}_I(t_I)$ and $\dot{y}_{II}(t_I)$ are connected with kink (*i.e.*, continuous and non-differentiable).

For t in the third interval $I_{III} = [t_{II}, t_{III}]$ with $t_{III} = t_{II} + \theta \approx 6.03$, we have $3n/v > \dot{y}_{II}(t - \theta) > -n/v$. Hence, successive integration implies that Equation (13) with $\Phi[\dot{y}_{II}(t - \theta)] = v \dot{y}_{II}(t - \theta)$ yields the trajectories described by

$$(G-III) \begin{cases} y_{III}(t) = e^{-\frac{1-\alpha}{\varepsilon}t} (\alpha_2^{III}t^2 + \alpha_1^{III}t + \alpha_0^{III}) \\ \dot{y}_{III}(t) = e^{-\frac{1-\alpha}{\varepsilon}t} (\beta_2^{III}t^2 + \beta_1^{III}t + \beta_0^{III}) \end{cases} \text{ for } t \in I_{III}$$

where

$$\begin{aligned} \alpha_2^{III} &= \frac{v}{\varepsilon} e^{\frac{1-\alpha}{\varepsilon}\theta} \frac{\beta_1^{II}}{2} \cdot 537.41, & \beta_2^{III} &= -\frac{1-\alpha}{\varepsilon} \alpha_2^{III} \approx -429,93, \\ \alpha_1^{III} &= \frac{v}{\varepsilon} e^{\frac{1-\alpha}{\varepsilon}\theta} (\beta_0^{II} - \theta\beta_1^{II}) \approx 5521.58, & \beta_1^{III} &= 2\alpha_2^{III} - \frac{1-\alpha}{\varepsilon} \alpha_1^{III} \approx 5521.68, \\ \alpha_0^{III} &\approx 14044.6, & \beta_0^{III} &= \alpha_1^{III} - \frac{1-\alpha}{\varepsilon} \alpha_0^{III} \approx -16794.2. \end{aligned}$$

Since $y_{II}(t_{II}) = y_{III}(t_{II})$ and $\dot{y}_{II}(t_{II}) = \dot{y}_{III}(t_{II})$ hold, the blue and red trajectories are continuous at $t = t_{II}$. The boundary values for the right endpoint of interval I_{III} are

$$y_{III}(t_{III}) \approx 0.55 \text{ and } \dot{y}_{III}(t_{III}) \approx 6.98.$$

As is seen in **Figure 4**, the red curve $\dot{y}_{III}(t)$ crosses the upper horizontal dotted line from below at $t_b \approx 5.19$ and $\dot{y}_{III}(t) < 3n/v$ for $t_{II} < t < t_b$. This crossing point is also denoted by the green dot.

In the fourth interval $I_{IV} = [t_{III}, t_{IV}]$ with $t_{IV} = t_b + \theta \approx 6.19$, Equation (13) with $\Phi[\dot{y}_{III}(t - \theta)] = v\dot{y}_{III}(t - \theta)$ determines the trajectories,

$$(G-IV) \begin{cases} y_{IV}(t) = e^{\frac{1-\alpha}{\varepsilon}t} (\alpha_3^{IV}t^3 + \alpha_2^{IV}t^2 + \alpha_1^{IV}t + \alpha_0^{IV}) \\ \dot{y}_{IV}(t) = e^{\frac{1-\alpha}{\varepsilon}t} (\beta_3^{IV}t^3 + \beta_2^{IV}t^2 + \beta_1^{IV}t + \beta_0^{IV}) \end{cases} \text{ for } t \in I_{IV}$$

where

$$\begin{aligned} \alpha_3^{IV} &= \frac{v}{\varepsilon} e^{\frac{1-\alpha}{\varepsilon}\theta} \frac{\beta_1^{III}}{3} \approx -1275.76, & \beta_3^{IV} &= -\frac{1-\alpha}{\varepsilon} \alpha_3^{IV} \approx 1020.61, \\ \alpha_2^{IV} &= \frac{v}{\varepsilon} e^{\frac{1-\alpha}{\varepsilon}\theta} \frac{\beta_1^{III} - \theta\beta_2^{III}}{2} \approx 28404.7, & \beta_2^{IV} &= 3\alpha_3^{IV} - \frac{1-\alpha}{\varepsilon} \alpha_2^{IV} \approx -26551, \\ \alpha_1^{IV} &= \beta_0^{III} - \theta\beta_1^{III} + \theta^2\beta_2^{III} \approx -202487, & \beta_1^{IV} &= 2\alpha_2^{IV} - \frac{1-\alpha}{\varepsilon} \alpha_1^{IV} \approx 218799, \\ \alpha_0^{IV} &\approx -467961, & \beta_0^{IV} &= \alpha_1^{IV} - \frac{1-\alpha}{\varepsilon} \alpha_0^{IV} \approx -576852. \end{aligned}$$

Since interval I_{IV} is very narrow, the right end point of I_{IV} is labelled at the upper part of **Figure 4** to avoid the notational congestion. Due to the continuity of the blue and red trajectories at $t = t_{III}$, $y_{III}(t_{III}) = y_{IV}(t_{III})$ and $\dot{y}_{III}(t_{III}) = \dot{y}_{IV}(t_{III})$ hold. The boundary values for the right end point of interval I_{IV} are calculated as

$$y_{IV}(t_{IV}) \approx 2.49 \text{ and } \dot{y}_{IV}(t_{IV}) \approx 16.01.$$

Since $\dot{y}_{IV}(t - \theta) > 3n/v$ holds in the fifth interval $I_V = [t_{IV}, t_V]$ where $t_V = t_c + \theta \approx 8.78$ and $t_c \approx 7.78$ solves $\dot{y}_V(t) = 3n/v$, Equation (13) with $\Phi[\dot{y}_{IV}(t - \theta)] = 3n$ gives the following forms of the solution and its time derivative,

$$(G-V) \begin{cases} y_V(t) = e^{\frac{1-\alpha}{\varepsilon}t} K_V + \frac{3n}{1-\alpha} \\ \dot{y}_V(t) = e^{\frac{1-\alpha}{\varepsilon}t} \left(-\frac{1-\alpha}{\varepsilon} K_V \right) \end{cases} \text{ for } t \in I_V$$

where $K_V \approx -2839.05$. The crossing point of the red curve with the upper horizontal dotted line at t_c is denoted by the green dot. The boundary values for the right end point of this interval are

$$y_V(t_V) \approx 19.97 \text{ and } \dot{y}_V(t_V) \approx 2.02.$$

Since $y_V(t - \theta) < 3n/v$ holds for t of the sixth interval $I_{VI} = [t_V, t_{VI}]$ with $t_{VI} = t_V + \theta \approx 9.78$, dynamic Equation (13) with $\varphi[\dot{y}_V(t - \theta)] = v\dot{y}_V(t - \theta)$ determines the following evolution of $y(t)$ and $\dot{y}(t)$:

$$(G-VI) \begin{cases} y_{VI}(t) = e^{-\frac{1-\alpha}{\varepsilon}t} (\alpha_1^{VI}t + \alpha_0^{VI}) \\ \dot{y}_{VI}(t) = e^{-\frac{1-\alpha}{\varepsilon}t} (\beta_1^{VI}t + \beta_0^{VI}) \end{cases} \text{ for } t \in I_{VI}$$

where

$$\begin{aligned} \alpha_1^{VI} &= -\frac{\nu(1-\alpha)}{\varepsilon^2} e^{\frac{1-\alpha}{\varepsilon}\theta} K_V \approx 20129, \\ \beta_1^{VI} &= -\frac{1-\alpha}{\varepsilon} \alpha_1^{VI} \approx -16175.2, \\ \alpha_0^{VI} &\approx -155088, \\ \beta_0^{VI} &= \alpha_1^{VI} - \frac{1-\alpha}{\varepsilon} \alpha_0^{VI} \approx 144289. \end{aligned}$$

The boundary values for the right end point of interval I_{VI} are

$$y_{VI}(t_{VI}) \approx 17.06 \text{ and } \dot{y}_{VI}(t_{VI}) \approx -5.56.$$

It is seen that the red curve crosses the lower horizontal dotted line from above at $t_d \approx 9.05$.

In the seventh interval $I_{VII} = [t_{VI}, t_{VII}]$ with $t_{VII} = t_d + \theta \approx 10.05$, applying successive integration to dynamic Equation (13) with $\varphi[\dot{y}_{VI}(t - \theta)] = v\dot{y}_{VI}(t - \theta)$ yields the forms of the solutions,

$$(G-VII) \begin{cases} y_{VII}(t) = e^{-\frac{1-\alpha}{\varepsilon}t} (\alpha_2^{VII}t^2 + \alpha_1^{VII}t + \alpha_0^{VII}) \\ \dot{y}_{VII}(t) = e^{-\frac{1-\alpha}{\varepsilon}t} (\beta_2^{VII}t^2 + \beta_1^{VII}t + \beta_0^{VII}) \end{cases} \text{ for } t \in I_{VII}$$

where

$$\begin{aligned} \alpha_2^{VII} &= \frac{\nu}{\varepsilon} e^{\frac{1-\alpha}{\varepsilon}\theta} \frac{\beta_1^{VI}}{2} \approx -71997, & \beta_2^{VII} &= -\frac{1-\alpha}{\varepsilon} \alpha_2^{VII} \approx 51597.63, \\ \alpha_1^{VII} &= \frac{\nu}{\varepsilon} e^{\frac{1-\alpha}{\varepsilon}\theta} (\beta_0^{VI} - \theta\beta_1^{VI}) \approx 142848.2, & \beta_1^{VII} &= 2\alpha_2^{VII} - \frac{1-\alpha}{\varepsilon} \alpha_1^{VII} \approx -128678, \\ \alpha_0^{VII} &\approx -704149.86, & \beta_0^{VII} &= \alpha_1^{VII} - \frac{1-\alpha}{\varepsilon} \alpha_0^{VII} \approx 706168. \end{aligned}$$

The boundary values for the right end point of interval I_{VII} are

$$y_{VII}(t_{VII}) \approx 13.82 \text{ and } \dot{y}_{VII}(t_{VII}) \approx -17.06.$$

Finally, in the eighth interval $I_{VIII} = [t_{VII}, t_E]$ with $t_E = t_{VII} + \theta \approx 11.05$, $\dot{y}_{VII}(t) < n/v$ for $t \in I_{VIII}$ implies dynamic Equation (5) with

$\varphi[\dot{y}_{VIII}(t-\theta)] = -n$ controls the trajectories,

$$(G-VIII) \begin{cases} y_{VIII}(t) = e^{\frac{1-\alpha}{\varepsilon}t} K_{VIII} - \frac{n}{1-\alpha} \\ \dot{y}_{VIII}(t) = e^{\frac{1-\alpha}{\varepsilon}t} \left(-\frac{1-\alpha}{\varepsilon} K_{VIII} \right) \end{cases} \text{ for } t \in I_{VIII}$$

where $K_{VIII} \approx 66133.90$. Notice that $y_{VIII}(t_E) = y_I(t_S)$ and $\dot{y}_{VIII}(t_E) = \dot{y}_I(t_S)$ hold. The length of the period is about 10 years.⁵ Very roughly speaking, the recovery period could be approximately 4.7 years from t_I to t_V and then the recession period is 5.3 years. The same cycle repeats itself for $t > t_E$.

4.2. Phase Plot

Calculating the boundary values of each interval I_i , we have the following set of points $(\dot{y}(t), y(t))$ in the phase diagram of **Figure 5**.

$$\begin{aligned} (S) &= (-7.62, 2.02) & (2) &= (-0.67, -6.66) & (3) &= (1.85, -5.69) \\ (4) &= (7.00, 0.55) & (5) &= (16.01, 2.49) & (6) &= (2.02, 19.97) \\ (7) &= (-5.56, 17.06) & (8) &= (-17.06, 13.82) & (E) &= (-7.62, 2.02) \end{aligned}$$

Point denoted by (S) and (E) is the starting point and the ending point of the cyclic oscillation, both of which are identical. Equation (5) with $d = -n$ governs decreasing movements from (S) to (2) and from (8) to (E) along the lower red line whereas Equation (5) with $d = 3n$ controls upward movements

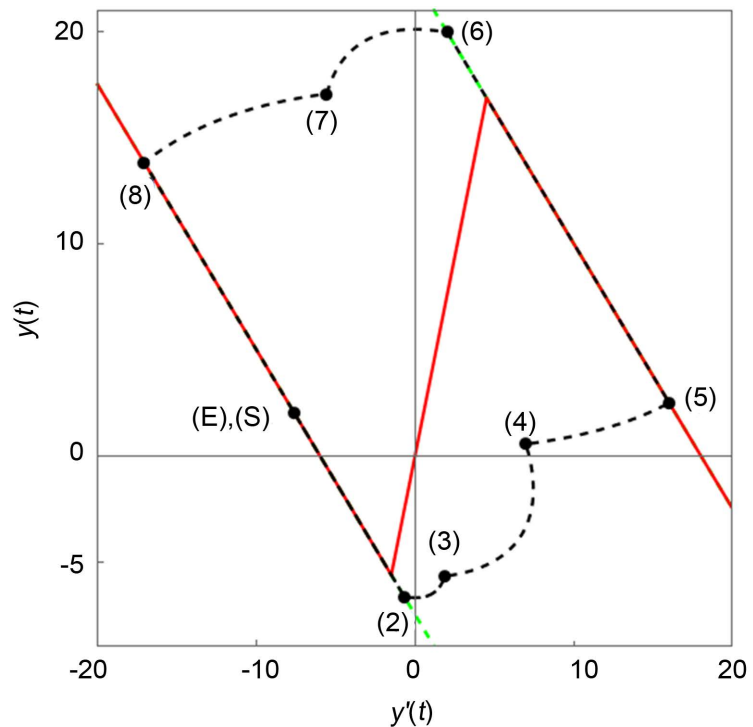


Figure 5. Phase diagram of Goodwin Equation (12).

⁵With the same parameter values but different initial values, [1] analytically obtained a 9 years cycle and [4] numerically got an 8.12 year cycle.

from (5) to (6) along the upper red line. On the other hand, movements from (2) to (5) and from (6) to (8) along the dotted curves between these two lines are described by Equation (13). The switching of dynamic equations occurs at the following points:

Point (2) at which Equation (5) with $d = -n$ is changed to Equation (13);

Point (5) at which Equation (13) to Equation (5) with $d = 3n$;

Point (6) at which Equation (5) with $d = 3n$ to Equation (13);

Point (8) at which Equation (13) to Equation (5) with $d = -n$;

Points (3), (4) and (7) at which Equations (13) have at different forms of $\Phi[\dot{y}(t-\theta)]$

We can verify the following.

Theorem 4 *The cyclic time trajectories of $y(t)$ and $\dot{y}(t)$ are continuous at these switching points.*

Proof. 1) At point (2) with $t = t_I$, $y_I(t)$ is connected to $y_{II}(t)$ and so is $\dot{y}_I(t)$ to $\dot{y}_{II}(t)$. Integral constant α_0^{II} of $y_{II}(t)$ is determined so as to solve $y_I(t_I) = y_{II}(t_I)$. Further $y_I(t)$ and $y_{II}(t)$ should satisfy the dynamic equations at $t = t_I$,

$$\begin{aligned} \varepsilon \dot{y}_I(t_I) + (1 - \alpha)y_I(t_I) &= -n, \\ \varepsilon \dot{y}_{II}(t_I) + (1 - \alpha)y_{II}(t_I) &= \nu \dot{y}_I(t_I - \theta). \end{aligned}$$

$\dot{y}_I(t_I - \theta) = \dot{y}_I(t_a)$ holds at $t_I = t_a + \theta$ and $\dot{y}_I(t_a) = -n/\nu$ by definition of t_a , both of which lead to $\nu \dot{y}_I(t_I - \theta) = -n$. Therefore the above two dynamic equations are identical and thus two solutions of these dynamic equations take the same values at $t = t_I$, namely, $y_I(t_I) = y_{II}(t_I)$ and $\dot{y}_I(t_I) = \dot{y}_{II}(t_I)$.

2) At point (5) with $t = t_{IV}$, $y_{IV}(t)$ is connected to $y_V(t)$ and so is $\dot{y}_{IV}(t)$ to $\dot{y}_V(t)$. Integral constant K_V of $y_{IV}(t)$ is determined so as to solve $y_{IV}(t_{IV}) = y_V(t_{IV})$. Further, $y_{IV}(t)$ and $y_V(t)$ should satisfy the dynamic equations at $t = t_{IV}$,

$$\begin{aligned} \varepsilon \dot{y}_{IV}(t_{IV}) + (1 - \alpha)y_{IV}(t_{IV}) &= \theta \dot{y}_{III}(t_{IV} - \theta), \\ \varepsilon \dot{y}_V(t_{IV}) + (1 - \alpha)y_{IV}(t_{IV}) &= 3n. \end{aligned}$$

$\dot{y}_{III}(t_{IV} - \theta) = \dot{y}_I(t_a)$ holds at $t_{IV} = t_b + \theta$ and $\dot{y}_{III}(t_b) = 3n/\nu$ by definition of t_b , both of which lead to $\theta \dot{y}_{III}(t_{IV} - \theta) = 3n$. Therefore the above two dynamic equations are identical and thus two solutions of these dynamic equations take the same values at $t = t_{IV}$, namely, $y_{IV}(t_{IV}) = y_V(t_{IV})$ and $\dot{y}_{IV}(t_{IV}) = \dot{y}_V(t_{IV})$. The same procedure applies for points (6) and (8).

3) At point (3) with $t = t_{II}$, $y_{II}(t)$ and $y_{III}(t)$ satisfy the dynamic equations

$$\begin{aligned} \varepsilon \dot{y}_{II}(t_{II}) + (1 - \alpha)y_{II}(t_{II}) &= \theta \dot{y}_I(t_{II} - \theta), \\ \varepsilon \dot{y}_{III}(t_{II}) + (1 - \alpha)y_{III}(t_{II}) &= \theta \dot{y}_{II}(t_{II} - \theta). \end{aligned}$$

$\dot{y}_I(t_{II} - \theta) = \dot{y}_I(t_I)$ and $\dot{y}_{II}(t_{II} - \theta) = \dot{y}_{II}(t_I)$ as $t_{II} = t_I + \theta$. From (i), we already have $\dot{y}_I(t_I) = \dot{y}_{II}(t_I)$. Further the integral constant α_1^{III} of $y_{III}(t)$ solves $y_{II}(t_{II}) = y_{III}(t_{II})$. Then substituting the second equation from the first

equation presents $\dot{y}_{II}(t_{II}) = \dot{y}_{III}(t_{II})$. The same procedure applies for Points (4) and (7).

This theorem confirms no jumps of the derivatives at the switching points of the dynamic system, implying the smooth time trajectory of national income just like observed business cycle. This is what [1] aims to obtain. So we summarize this results as follows:

Theorem 5 *If the initial value y_0 of the initial function and the length of delay θ are selected such as $y_0 < y_0^{\min}(\theta)$ or $y_0 > y_0^{\max}(\theta)$, then the delay model can generate smooth oscillations of national income.*

5. Sawtooth Oscillations

Under Assumptions 1 and 2 with $y_0^s = -2$, **Figure 6** illustrates trajectories of $y(t)$ (blue curve) and $\dot{y}(t)$ (red curve) for $t \in [0, 5]$. The blue trajectory has kinks and the red trajectory jumps at $t_i = n\theta$. These are initial parts of the trajectories that eventually converge to sawtooth oscillations. The shapes of these trajectories are different from those in **Figure 2** and **Figure 4**.

It has been pointed out by [4] that the delay model also gives rise to sawtooth-like oscillations.⁶ Our main aim of this section is to analytically reproduce these numerical results to understand why a trajectory $y(t)$ has kinks and its derivative $\dot{y}(t)$ makes jumps. To this end, we start to divide the interval $I = [0, 5]$ into five subintervals with respect to the length of delay θ ,

$$I_i = [t_{i-1}, t_i] \text{ for } i = 1, 2, 3, 4, 5$$

where $t_{i-1} = i - 1$ and $t_i = t_{i-1} + \theta$ with $\theta = 1$. Detailed derivations of the forms of $y(t)$ and $\dot{y}(t)$ in each interval are presented in Appendix II.

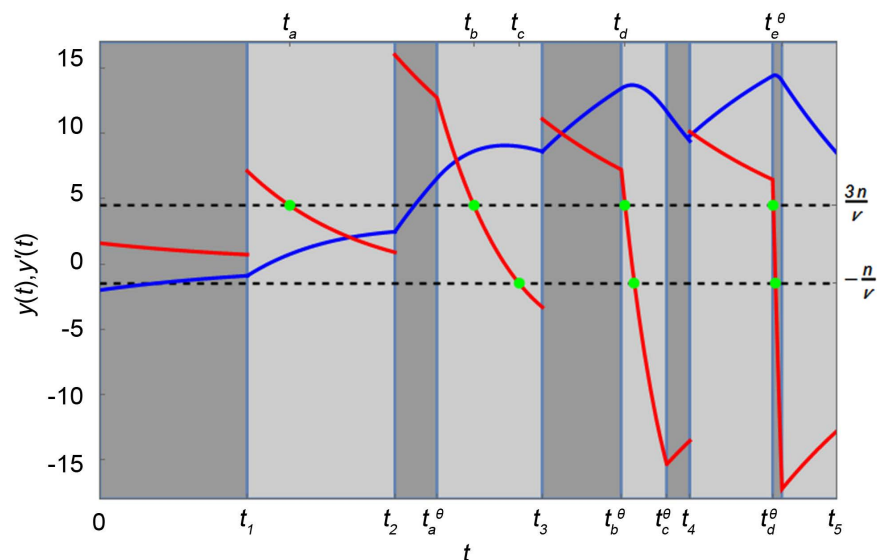


Figure 6. Time trajectories of $y(t)$ (blue) and $y'(t)$ (red) for $0 \leq t \leq 5$.

⁶More precisely, [4] found at least twenty five other limit cycles were also solution to the delay model with the same parameter values. Further it was indicated that there were an infinite number of additional solutions.

5.1. Time Trajectories

The constant initial function $\Phi(t - \theta) = -2$ for $t \in I_1 = [t_0, t_1]$ is selected. The dynamic Equation (13) with $\varphi[\Phi(t - \theta)] = 0$ yields the following forms of the solution and its derivative

$$(S-I) \begin{cases} y_1(t) = e^{\frac{1-\alpha}{\varepsilon} t} K_1 \text{ with } K_1 = -2, \\ \dot{y}_1(t) = e^{\frac{1-\alpha}{\varepsilon} t} \left(-\frac{1-\alpha}{\varepsilon} K_1 \right). \end{cases}$$

The boundary values for the end points of interval I_1 are

$$y_1(t_0) \approx -2, \dot{y}_1(t_0) \approx 1.6 \text{ and } y_1(t_1) \approx -0.897, \dot{y}_1(t_1) \approx 0.719.$$

In the second interval $I_2 = [t_1, t_2]$, solving (13) with $\varphi[\dot{y}_1(t - \theta)] = \nu \dot{y}_1(t - \theta)$ by successive integration yields the following forms

$$(S-II) \begin{cases} y_2(t) = e^{\frac{1-\alpha}{\varepsilon} t} (\alpha_1'' t + \alpha_0'') \\ \dot{y}_2(t) = e^{\frac{1-\alpha}{\varepsilon} t} (\beta_1'' t + \beta_0'') \end{cases}$$

where

$$\begin{aligned} \alpha_1'' &= -\frac{k(1-\alpha)}{\varepsilon^2} K_1 e^{\frac{1-\alpha}{\varepsilon} \theta} \approx 14.244, \\ \beta_1'' &= -\frac{k(1-\alpha)^2}{\varepsilon^3} e^{\frac{1-\alpha}{\varepsilon} \theta} K_1 \approx -11.395, \\ \alpha_0'' &\approx -16.244, \\ \beta_0'' &= -\frac{1-\alpha}{\varepsilon} \left(\frac{k}{\varepsilon} e^{\frac{1-\alpha}{\varepsilon} \theta} K_1 + K_2 \right) \approx 27.238. \end{aligned}$$

Integral constant α_0'' is determined so as to satisfy $y_2(t_1) = y_1(t_1)$, implying the continuity of the blue curve at t_1 . The discontinuity of the red curve at that point can be shown in the same way as in the case of Goodwin cycle. The solutions $y_1(t_1)$ and $y_2(t_1)$ satisfy the corresponding dynamic equations at $t = t_1$,

$$\begin{aligned} \varepsilon \dot{y}_1(t_1) + (1-\alpha) y_1(t_1) &= 0, \\ \varepsilon \dot{y}_2(t_1) + (1-\alpha) y_2(t_1) &= \nu \dot{y}_1(t_1 - \theta) \end{aligned}$$

where $t_1 = t_0 + \theta$ and $t_0 = 0$ implying that $\dot{y}_1(t_1 - \theta) = \dot{y}_1(0) > 0$. Subtracting the first equation from the second equation presents

$$\dot{y}_2(t_1) - \dot{y}_1(t_1) = \frac{\nu}{\varepsilon} \dot{y}_1(0) > 0 \text{ or } \dot{y}_2(t_1) > \dot{y}_1(t_1).$$

The last inequality confirms the discontinuity of the red curve at $t = t_1$. The boundary values for the end points of interval I_2 are

$$y_2(t_1) \approx -0.897, \dot{y}_2(t_1) \approx 7.119 \text{ and } y_2(t_2) \approx 2.472, \dot{y}_2(t_2) \approx 0.898.$$

It is then numerically confirmed that

$$y_1(t_1) = y_2(t_1) \Rightarrow \text{continuity of the blue curve at } t = t_1,$$

$$\dot{y}_1(t_0) \neq \dot{y}_2(t_1) \Rightarrow \text{discontinuity of the red curve at } t = t_1.$$

As shown in the Appendix II, t_a is the value at which the red curve crosses the upper horizontal dotted line once from above and divides the interval $I_3 = [t_2, t_3]$ into two subintervals, $I_3^a = [t_2, t_a^\theta]$ and $I_3^b = [t_a^\theta, t_3]$ where $t_a^\theta = t_a + \theta$. So we derive a solution of the differential equation in each interval. In interval I_3^a Equation (5) with $d = 3n$ presents the forms of $y(t)$ and $\dot{y}(t)$:

$$(S-IIIa) \begin{cases} y_3^a(t) = e^{-\frac{1-\alpha}{\varepsilon}t} K_3 + \frac{3n}{1-\alpha}, \\ \dot{y}_3^a(t) = -\frac{1-\alpha}{\varepsilon} K_3 e^{-\frac{1-\alpha}{\varepsilon}t}, \end{cases}$$

where solving $y_3^a(t_2) = y_2(t_2)$ gives constant value $K_3 \approx -99.20$. The boundary values for the end points of interval I_3^a are

$$y_3^a(t_2) \approx 2.472, \dot{y}_3^a(t_2) \approx 16.023 \text{ and } y_3^a(t_a^\theta) \approx 6.565, \dot{y}_3^a(t_a^\theta) \approx 12.748$$

where the continuity of the blue curve and the discontinuity of the red curve at $t = t_2$ are also numerically confirmed,

$$y_2(t_2) = y_3^a(t_2) \text{ and } \dot{y}_2(t_2) \neq \dot{y}_3^a(t_2).$$

On the other hand, in interval I_3^b , Equation (13) with $\varphi[\dot{y}_2(t - \theta)] = \nu \dot{y}_2(t - \theta)$ yields the solution and its derivative,

$$(S-IIIb) \begin{cases} y_3^b(t) = e^{-\frac{1-\alpha}{\varepsilon}t} (\alpha_2^{\text{III}} t^2 + \alpha_1^{\text{III}} t + \alpha_0^{\text{III}}) \\ \dot{y}_3^b(t) = e^{-\frac{1-\alpha}{\varepsilon}t} (\beta_2^{\text{III}} t^2 + \beta_1^{\text{III}} t + \beta_0^{\text{III}}) \end{cases}$$

where

$$\alpha_2^{\text{III}} = \frac{k}{\varepsilon} e^{-\frac{1-\alpha}{\varepsilon}\theta} \frac{\beta_1^{\text{II}}}{2} \approx -50.719, \quad \beta_2^{\text{III}} = -\frac{1-\alpha}{\varepsilon} \alpha_2^{\text{III}} \approx -22.79,$$

$$\alpha_1^{\text{III}} = \frac{k}{\varepsilon} e^{-\frac{1-\alpha}{\varepsilon}\theta} (\beta_0^{\text{II}} - \theta \beta_1^{\text{II}}) \approx 343.918, \quad \beta_1^{\text{III}} = 2\alpha_2^{\text{III}} - \frac{1-\alpha}{\varepsilon} \alpha_1^{\text{III}} \approx -255.97$$

$$\alpha_0^{\text{III}} = -480.253, \quad \beta_0^{\text{III}} = \alpha_1^{\text{III}} - \frac{1-\alpha}{\varepsilon} \alpha_0^{\text{III}} \approx 559.71.$$

The boundary values for the end points of interval I_3^b are

$$y_3^b(t_a^\theta) \approx 6.565, \dot{y}_3^b(t_a^\theta) \approx 12.748 \text{ and } y_3^b(t_3) \approx 8.621, \dot{y}_3^b(t_3) \approx -3.309$$

where the blue and red curves are confirmed to be continuous at $t = t_a^\theta$,

$$y_3^a(t_a^\theta) = y_3^b(t_a^\theta) \text{ and } \dot{y}_3^a(t_a^\theta) = \dot{y}_3^b(t_a^\theta).$$

Due to the values of t_b and t_c obtained in the Appendix II, interval $I_4 = [t_3, t_4]$ is divided into three subintervals $I_4^a = [t_3, t_b^\theta]$, $I_4^b = [t_b^\theta, t_c^\theta]$ and $I_4^c = [t_c^\theta, t_4]$ by $t_b^\theta = t_b + \theta$ and $t_c^\theta = t_c + \theta$. Since $\varphi[\dot{y}_3(t - \theta)] = \varphi[\dot{y}_4(t - \theta)] = 3n$ for $t \in I_4^a$, Equation (5) with $d = 3n$ yields

the solution of the differential equation and its derivative

$$(S-VIa) \begin{cases} y_4^a(t) = e^{\frac{1-\alpha}{\varepsilon}t} K_4^a + \frac{3n}{1-\alpha} & \text{with } K_4^a \approx -152.994, \\ \dot{y}_4^a(t) = e^{\frac{1-\alpha}{\varepsilon}t} \left(-\frac{1-\alpha}{\varepsilon} K_4^a \right) & \text{with } -\frac{1-\alpha}{\varepsilon} K_4^a \approx 122.395. \end{cases}$$

The boundary values for the end points of interval I_4^a are

$$y_4^a(t_3) \approx 8.621, \dot{y}_4^a(t_3) \approx 11.103 \text{ and } y_4^a(t_b^\theta) \approx 13.456, \dot{y}_4^a(t_b^\theta) \approx 7.236$$

where the blue curve is continuous and the red curve jumps at $t = t_3$,

$$y_3^b(t_3) = y_4^a(t_3) \text{ and } \dot{y}_3^b(t_3) \neq \dot{y}_4^a(t_3).$$

In I_4^b , Equation (13) with $\varphi[\dot{y}_4^a(t-\theta)] = v\dot{y}_4^a(t-\theta)$ gives the solution and its derivative

$$(S-IVb) \begin{cases} y_4^b(t) = e^{\frac{1-\alpha}{\varepsilon}t} \{ \alpha_3^{IV} t^3 + \alpha_2^{IV} t^2 + \alpha_1^{IV} t + \alpha_0^{IV} \} \\ \dot{y}_4^b(t) = e^{\frac{1-\alpha}{\varepsilon}t} \{ \beta_3^{IV} t^3 + \beta_2^{IV} t^2 + \beta_1^{IV} t + \beta_0^{IV} \} \end{cases}$$

where

$$\begin{aligned} \alpha_3^{IV} &= \frac{k}{\varepsilon} e^{\frac{1-\alpha}{\varepsilon}\theta} \frac{\beta_2^{III}}{3} \approx 180.604, & \beta_3^{IV} &= -\frac{1-\alpha}{\varepsilon} \alpha_3^{IV} \approx -96.322, \\ \alpha_2^{IV} &= \frac{k}{\varepsilon} e^{\frac{1-\alpha}{\varepsilon}\theta} \frac{\beta_1^{III} - 2\theta\beta_2^{III}}{2} \approx -2037.36, & \beta_2^{IV} &= 3\alpha_3^{IV} - \frac{1-\alpha}{\varepsilon} \alpha_2^{IV} \approx 1991.1, \\ \alpha_1^{IV} &= \frac{k}{\varepsilon} e^{\frac{1-\alpha}{\varepsilon}\theta} (\beta_0^{III} - \theta\beta_1^{III} + \theta^2\beta_2^{III}) \approx 10195.4, & \beta_1^{IV} &= 2\alpha_2^{IV} - \frac{1-\alpha}{\varepsilon} \alpha_1^{IV} \approx -12231, \\ \alpha_0^{IV} &\approx -15672.428, & \beta_0^{IV} &= \alpha_1^{IV} - \frac{1-\alpha}{\varepsilon} \alpha_0^{IV} \approx 22733.3. \end{aligned}$$

The boundary values for the end points of interval I_4^b are

$$y_4^b(t_b^\theta) \approx 13.456, \dot{y}_4^b(t_b^\theta) \approx 7.236 \text{ and } y_4^b(t_c^\theta) \approx 11.677, \dot{y}_4^b(t_c^\theta) \approx -15.342$$

where the blue and red curves are continuous at $t = t_b^\theta$,

$$y_4^a(t_b^\theta) = y_4^b(t_b^\theta) \text{ and } \dot{y}_4^a(t_b^\theta) = \dot{y}_4^b(t_b^\theta).$$

Since $\varphi[\dot{y}_4^b(t-\theta)] = -n$ for $t \in I_4^c$ Equation (5) with $d = -n$ yields the solution and its derivative

$$(S-IVc) \begin{cases} y_4^c(t) = e^{\frac{1-\alpha}{\varepsilon}t} K_7 - \frac{n}{1-\alpha} & \text{with } K_7 \approx 415.092 \\ \dot{y}_4^c(t) = e^{\frac{1-\alpha}{\varepsilon}t} \left(-\frac{1-\alpha}{\varepsilon} K_7 \right) & \text{with } -\frac{1-\alpha}{\varepsilon} K_7 \approx -340.074 \end{cases}$$

The boundary values for the end points of interval I_4^c are

$$y_4^c(t_c^\theta) \approx 11.677, \dot{y}_4^c(t_c^\theta) \approx -15.342 \text{ and } y_4^c(t_4) \approx 9.420, \dot{y}_4^c(t_4) \approx -13.536$$

where the blue and red curves are continuous at $t = t_c^\theta$

$$y_4^b(t_c^\theta) = y_4^c(t_c^\theta) \text{ and } \dot{y}_4^b(t_c^\theta) = \dot{y}_4^c(t_c^\theta).$$

Due to the crossing values t_d and t_e obtained in the Appendix II, interval $I_5 = [t_4, t_5]$ is divided into three subintervals $I_5^a = [t_4, t_d^\theta]$ and $I_5^b = [t_d^\theta, t_e^\theta]$ and $I_5^c = [t_e^\theta, t_5]$ by $t_d^\theta = t_d + \theta$ and $t_e^\theta = t_e + \theta$. Since $\varphi[\dot{y}_4^b(t - \theta)] = \varphi[\dot{y}_4^c(t - \theta)] = 3n$ for $t \in I_5^a$, Equation (5) with $d = 3n$ implies the solution and its derivative,

$$(S-Va) \begin{cases} y_5^a(t) = e^{-\frac{1-\alpha}{\varepsilon}t} K_8 + \frac{3n}{1-\alpha} & \text{with } K_8 \approx -320.88 \\ \dot{y}_5^a(t) = e^{-\frac{1-\alpha}{\varepsilon}t} \left(-\frac{1-\alpha}{\varepsilon} K_8 \right) & \text{with } -\frac{1-\alpha}{\varepsilon} K_8 \approx 256.704 \end{cases}$$

The boundary values for the end points of interval I_5^a are

$$y_5^a(t_4) \approx 9.420, \dot{y}_5^a(t_4) \approx 10.464 \text{ and } y_5^a(t_d^\theta) \approx 14.150, \dot{y}_5^a(t_d^\theta) \approx 6.680$$

where the blue curve of $y(t)$ is continuous but kinked at $t = t_4$ and accordingly, the red curve of $\dot{y}(t)$ jumps at $t = t_4$,

$$y_4^c(t_4) = y_5^a(t_4) \text{ and } \dot{y}_4^c(t_4) \neq \dot{y}_5^a(t_4)$$

In I_5^b , Equation (13) with $\varphi[\dot{y}_4^a(t - \theta)] = \nu \dot{y}_4^a(t - \theta)$ yields the solution and its derivative

$$(S-Vb) \begin{cases} y_5^b(t) = e^{-\frac{1-\alpha}{\varepsilon}t} \{ \alpha_4^V t^4 + \alpha_3^V t^3 + \alpha_2^V t^2 + \alpha_1^V t + \alpha_0^V \} \\ \dot{y}_5^b(t) = e^{-\frac{1-\alpha}{\varepsilon}t} \{ \beta_4^V t^4 + \beta_3^V t^3 + \beta_2^V t^2 + \beta_1^V t + \beta_0^V \} \end{cases}$$

where

$$\begin{aligned} \alpha_4^V &= \frac{k}{\varepsilon} e^{-\frac{1-\alpha}{\varepsilon}\theta} \frac{\beta_3^{IV}}{3} \approx -214.369, \beta_4^V = -\frac{1-\alpha}{\varepsilon} \alpha_4^V \approx 171.495, \\ \alpha_3^V &= \frac{k}{\varepsilon} e^{-\frac{1-\alpha}{\varepsilon}\theta} \frac{\beta_2^{IV} - 3\theta\beta_3^{IV}}{3} \approx 6765.83, \beta_3^V = 4\alpha_4^V - \frac{1-\alpha}{\varepsilon} \alpha_3^V \approx -9270.135, \\ \alpha_2^V &= \frac{k}{\varepsilon} e^{-\frac{1-\alpha}{\varepsilon}\theta} \frac{\beta_1^{IV} - 2\theta\beta_2^{IV} + 3\theta^2\beta_3^{IV}}{2} \approx -73452.5, \\ \beta_2^V &= 3\alpha_3^V - \frac{1-\alpha}{\varepsilon} \alpha_2^V \approx 79059.451, \\ \alpha_1^V &= \frac{k}{\varepsilon} e^{-\frac{1-\alpha}{\varepsilon}\theta} (\beta_0^{IV} - \theta\beta_1^{IV} + \theta^2\beta_2^{IV} - \theta^3\beta_3^{IV}) \approx 329841, \\ \beta_1^V &= 2\alpha_2^V - \frac{1-\alpha}{\varepsilon} \alpha_1^V \approx -410777.286, \\ \alpha_0^V &= K_9 \approx -525028.550, \\ \beta_0^V &= \alpha_1^V - \frac{1-\alpha}{\varepsilon} \alpha_0^V \approx 749863.287. \end{aligned}$$

The boundary values for the end points of interval I_5^b are

$$y_5^b(t_d^\theta) \approx 14.150, \dot{y}_5^b(t_d^\theta) \approx 6.680 \text{ and } y_5^b(t_e^\theta) \approx 13.793, \dot{y}_5^b(t_e^\theta) \approx -17.034.$$

Since $\varphi[\dot{f}_4^c(t-\theta)] = -n$ for $t \in I_5^c$, Equation (5) with $d = -n$ yields the solution and its derivative

$$(S-Vc) \begin{cases} y_5^c(t) = e^{\frac{1-\alpha}{\varepsilon}t} K_{10} - \frac{n}{1-\alpha} & \text{with } K_{10} \approx 860.508 \\ \dot{y}_5^c(t) = e^{\frac{1-\alpha}{\varepsilon}t} \left(-\frac{1-\alpha}{\varepsilon} K_{10} \right) & \text{with } -\frac{1-\alpha}{\varepsilon} K_{10} \approx -688.406 \end{cases}$$

The boundary values for the end points of interval I_5^c are

$$y_5^c(t_e^\theta) \approx 13.793, \dot{y}_5^c(t_e^\theta) \approx -17.034 \text{ and } y_5^c(t_5) \approx 8.267, \dot{y}_5^c(t_5) \approx -12.614$$

where the blue and red curves are continuous at $t = t_e^\theta$,

$$y_5^b(t_e^\theta) = y_5^c(t_e^\theta) \text{ and } \dot{y}_5^b(t_e^\theta) = \dot{y}_5^c(t_e^\theta).$$

Notice that the red curves in intervals, I_3, I_4 and I_5 intersect the upper and lower horizontal dotted curves and a difference between t -values is getting smaller,

$$t_c - t_b \approx 0.308, t_d - t_e \approx 0.063 \text{ and } t_f - t_g \approx 0.015.$$

As seen above, the delay differential Equation (13) describes dynamic behavior of $y(t)$ for $t \in I_k^b$ for $k = 3, 4, 5$ while the linear ordinary Equation (5) determines the form of $y(t)$ for $t \in I_k^a$ or I_k^c . For $k \geq 6$, the same types of the solutions are obtained and the size of I_k^b shrinks, implying that as k increases, the resultant shape of the solution form of $y(t)$ approaches the sawtooth shape at whose vertices $\dot{y}(t)$ jumps.

5.2. Phase Plot

We now turn attention to the phase diagram in the $(\dot{y}(t), y(t))$ plane. The boundary values of each trajectory that have been obtained are summarized in the following table and plotted in **Figure 7**. The red curves are the locus of $y(t) = f[\dot{y}(t-\theta)]$ and the green parallelogram is a sawtooth limit cycle. Black dotted curve connects the boundary values. The following points are shown in **Figure 7**:

- | | | |
|------------------------|------------------------|-----------------------|
| (1) = (1.6, -2) | (2) = (0.72, -0.90) | (3) = (7.12, -0.90) |
| (4) = (0.90, 2.47) | (5) = (16.02, 2.4) | (6) = (12.75, 6.57) |
| (7) = (-3.31, 8.62) | (8) = (11.10, 8.62) | (9) = (7.24, 13.46) |
| (10) = (-15.34, 11.68) | (11) = (-13.54, 9.42) | (12) = (10.46, 9.42) |
| (13) = (6.68, 14.15) | (14) = (-17.03, 13.79) | (15) = (-12.61, 8.27) |

Point (1) is the starting point of interval I_1 at $t = 0$ and the delay Equation (13) transports it to point (2) at $t = 1$. At the beginning of the second interval I_2 , $\dot{y}(t)$ jumps, which makes the horizontal move of point (2) to point (3) that arrives at point (4) at the end of I_2 . At the beginning of the third interval I_3 , $\dot{y}(t)$ jumps again and point (4) horizontally shifts to point (5) at which the dynamic system is changed to the linear Equation (5) with $d = 3n$ making a move along the upper downward line to point (6) as t proceeds from $t = t_2$ to

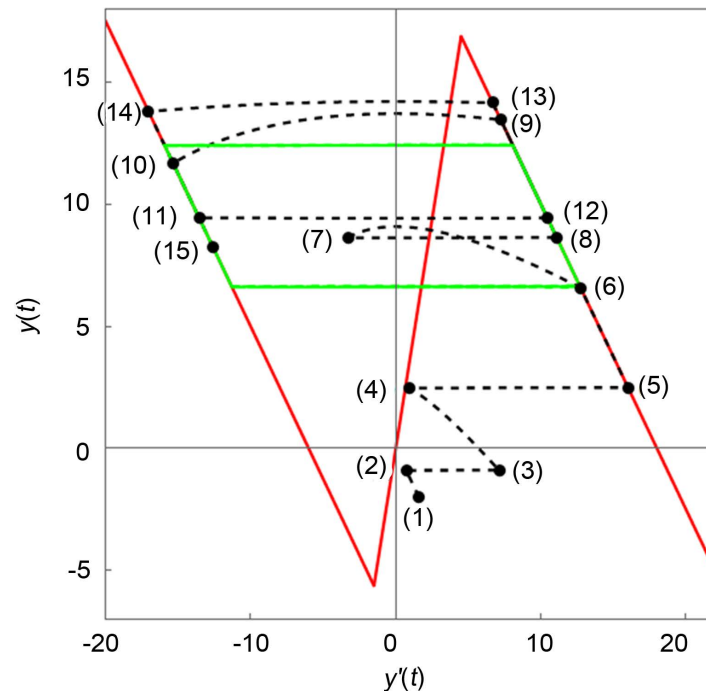


Figure 7. Phase diagram of sawtooth oscillation.

$t = t_a^\theta$. The dynamic system is changed back to the delay equation at $t = t_a^\theta$ and then the dotted trajectory leaves the upper red curve heading to point (7). This is because for $t \in [t_a^\theta, t_3]$, the delay equation with $\dot{y}(t - \theta) \in I_M$ controls dynamic behavior. On the way, the $\dot{y}(t)$ curve crosses the upper and lower horizontal dotted curves as seen in **Figure 6**. The move reaches point (7) at the end of I_3 and jumps to point (8) at the beginning of interval I_4 in which we see signs of sawtooth oscillations. Two intersections obtained in interval I_3 causes two changes of the dynamic system; the linear Equation (5) with $d = 3n$ governs the movement from point (8) to point (9) and the delay Equation (13) controls the movement from point (9) to point (10) and then the system is changed to the linear Equation (5) with $d = -n$ managing the movement along the lower downward line from point (10) to point (11). At the beginning of interval I_5 , a jump from point (11) to point (12) occurs and the further movement along the upper red line to point (13) is controlled by the linear equation with $d = 3n$, point (13) to point (14) by the delay equation and point (14) to point (15) by the linear equation with $d = -n$. Point (15) jumps to a point on the upper red line and the dynamic system change occurs as well in I_k for integer $k \geq 6$ as in I_5 . By doing so, the trajectory gradually approaches to the green sawtooth limit cycle as time goes on. It is noticed that a jump occurs at the local maximum or minimum point in the non-delay model whereas even at the middle of these boundary values in the delay model.

6. Concluding Remarks

This paper presented Goodwin's nonlinear accelerator model augmented with

investment delay in continuous time scales. Assuming a piecewise linear investment function and specifying the values of the model's parameters, explicit forms of sawtooth oscillations were derived when the initial value of the constant initial function was selected in the neighborhood of the steady state. Otherwise the same was done for Goodwin oscillation. With these numerical results, the paper exhibited valuable insights into the macro dynamics of market economies: the delay nonlinear accelerator-multiplier mechanism can be a source of various types of business cycles; economies starting in the neighborhood of the steady state could achieve regular ups and downs while economies starting away from the steady state presented persistent and irregular cycles.

References

- [1] Goodwin, R. (1951) The Nonlinear Accelerator and the Persistence of Business Cycles. *Econometrica*, **19**, 1-17. <https://doi.org/10.2307/1907905>
- [2] Matsumoto, A. and Szidarovszky, F. (2018) Goodwin Accelerator Model Revisited with Fixed Time Delays. *Communications in Nonlinear Science and Numerical Simulation*, **58**, 233-248. <https://doi.org/10.1016/j.cnsns.2017.06.024>
- [3] Matsumoto, A. (2009) Note on Goodwin's Nonlinear Acceleration Model with an Investment Delay. *Journal of Economic Dynamics and Control*, **33**, 832-842. <https://doi.org/10.1016/j.jedc.2008.08.013>
- [4] Strotz, R., McAnulty, J. and Naines, J. (1953) Goodwin's Non Linear Theory of the Business Cycle: An Electro-Analog Solution. *Econometrica*, **2**, 390-411. <https://doi.org/10.2307/1905446>
- [5] Antonova, A., Reznik, S. and Todorv, M. (2013) Relaxation Oscillation Properties in Goodwin's Business Cycle Model. *International Journal of Computational Economics and Econometrics*, **3**, 390-411. <https://doi.org/10.1504/IJCEE.2013.058495>
- [6] Freedman, H. and Kuang, Y. (1991) Stability Switches in Linear Scalar Neutral Delay Equations. *Funkcialaj Ekvacioj*, **34**, 187-209.

Appendix I

In this Appendix, we provide mathematical underpinnings for Goodwin oscillations. Since the investment delay could make $y(t)$ kinked and $\dot{y}(t)$ discontinuous at $t_n = n\theta$ for integer n , the time interval for $t \geq 0$ is reconstructed as the union of unit intervals $I_n = [t_n, t_{n+1}]$ for n and then a dynamic equation defined over interval I_n is solved to obtain explicit forms of time trajectory and its derivative. Dynamic equation is solved with successive integration in which an initial point or function is the solution of dynamic equation defined in the proceeding subinterval.

Interval 0: $I_0 = [t_0, t_1]$ where $t_0 = 0$ and $t_1 = 1$.

The initial function $\Phi(t - \theta)$ determines dynamics for $t \leq 0$. Since $\varphi[\dot{\Phi}(t - \theta)] = 0$ by Assumption 2, solving $\varepsilon \dot{y}(t) + (1 - \alpha)y(t) = 0$ presents explicit forms of the solution and its derivative

$$y_0(t) = e^{\frac{1-\alpha}{\varepsilon}t} K_0 \text{ and } \dot{y}_0(t) = e^{\frac{1-\alpha}{\varepsilon}t} \left(-\frac{1-\alpha}{\varepsilon} K_0 \right) \text{ with } K_0 = \frac{3n}{\nu}.$$

and as can be seen in **Figure 4**, the red curve is below the lower dotted line or

$$\dot{y}_0(t) < -\frac{n}{\nu} \text{ for } t \in I_0. \tag{A-1}$$

Derivation of (G-I)

Interval 1: $I_1 = [t_1, t_2]$ where $t_2 = 2$.

(A-1) implies $\varphi[\dot{y}_0(t - \theta)] = -n$ for $t \in I_1$ and then (8) with $d = -n$ are

$$y_1(t) = e^{\frac{1-\alpha}{\varepsilon}t} K_1 + \left(-\frac{n}{1-\alpha} \right) \text{ and } \dot{y}_1(t) = e^{\frac{1-\alpha}{\varepsilon}t} \left(-\frac{1-\alpha}{\varepsilon} K_1 \right)$$

where solving $y_0(t_1) = y_1(t_1)$ gives

$$K_1 = K_0 + \frac{n}{1-\alpha} e^{\frac{1-\alpha}{\varepsilon}t_1} \approx 21.19.$$

and the following holds,

$$\dot{y}_1(t) < -\frac{n}{\nu} \text{ for } t \in I_1. \tag{A-2}$$

Intervals 2 and 3: $I_i = [t_i, t_{i+1}]$ where $t_{i+1} = t_i + \theta$ for $i = 2, 3$.

In the same way as in interval I_1 , (8) with $d = -n$ leads to the identical forms of $y_i(t)$ and $\dot{y}_i(t)$ for $t \in I_i$ as the ones defined in I_1 ,

$$y_i(t) = y_1(t) \text{ and } \dot{y}_i(t) = \dot{y}_1(t) \text{ with } K_i = K_1.$$

Notice that the red curve crosses the lower dotted horizontal line from below in interval I_3 . Solving $\dot{y}_3(t) = -n/\nu$ for t gives

$$t_a \approx 3.03$$

with which the following inequalities hold

$$\dot{y}_3(t) < -\frac{n}{\nu} \text{ for } t < t_a \text{ and } -\frac{n}{\nu} < \dot{y}_3(t) < \frac{3n}{\nu} \text{ for } t_a < t \leq t_4. \tag{A-3}$$

Interval 4: $I_4 = [t_4, t_5]$ where $t_4 = 4$ and $t_5 = 5$.

Due to (A-3), $t_I = t_a + \theta \approx 4.03$ divides interval I_4 into two subintervals, $I_4^a = [t_4, t_I]$ and $I_4^b = [t_I, t_5]$. First, (2) with $\varphi[\dot{y}_3(t - \theta)] = -n$ for $t \in I_4^a$ presents the same forms

$$y_4^a(t) = y_1(t) \text{ and } \dot{y}_4^a(t) = \dot{y}_1(t) \text{ with } K_4^a = K_1.$$

So far we have seen that in $I_I = I_1 \cup I_2 \cup I_3 \cup I_4^a = [t_s, t_I]$ with $t_s = t_1$, a time trajectory of $y(t)$ is described by

$$y_I(t) = e^{-\frac{1-\alpha}{\varepsilon}t} K_I + \left(-\frac{n}{1-\alpha}\right)$$

where $y_I(t) = y_1(t)$ and $K_I = K_1$. A form of $\dot{y}_I(t)$ is obtained by time-differentiating $y_I(t)$ and is identical with $\dot{y}_1(t)$. $y_I(t)$ and $\dot{y}_I(t)$ construct system (G-I) defined in Section 4.1.

Derivation of (G-II)

On the other hand for $t \in I_4^b$, the investment is delayed and (12) with $\varphi[\dot{y}_3(t - \theta)] = v\dot{y}_3(t - \theta)$ is written as

$$\dot{y}(t) + \frac{1-\alpha}{\varepsilon}y(t) = \frac{v}{\varepsilon}e^{-\frac{1-\alpha}{\varepsilon}(t-\theta)}\left(-\frac{1-\alpha}{\varepsilon}K_3\right).$$

Multiplying both sides by the term $e^{\frac{1-\alpha}{\varepsilon}t}$ and arranging the terms present

$$\frac{d}{dt}\left[y(t)e^{\frac{1-\alpha}{\varepsilon}t}\right] = e^{\frac{1-\alpha}{\varepsilon}t}\left(-\frac{v(1-\alpha)}{\varepsilon^2}K_3e^{-\frac{1-\alpha}{\varepsilon}\theta}e^{\frac{1-\alpha}{\varepsilon}t}\right).$$

Integrating both sides yields

$$y(t)e^{\frac{1-\alpha}{\varepsilon}t} = \left(-\frac{v(1-\alpha)}{\varepsilon^2}K_3e^{-\frac{1-\alpha}{\varepsilon}\theta}\right)t + K_4^b.$$

Thus the form of the solution is

$$y_4^b(t) = e^{-\frac{1-\alpha}{\varepsilon}t}\left(\alpha_1^{iv}t + \alpha_0^{iv}\right)$$

where

$$\alpha_1^{iv} = -\frac{v(1-\alpha)}{\varepsilon^2}K_3e^{-\frac{1-\alpha}{\varepsilon}\theta} \text{ and } \alpha_0^{iv} = K_4^b.$$

The integral constant K_4^b is obtained by solving $y_4^a(t_I) = y_4^b(t_I)$,

$$K_4^b \approx 440.938.$$

The derivative of $y(t)$ is

$$\dot{y}_4^b(t) = e^{-\frac{1-\alpha}{\varepsilon}t}\left(\beta_1^{iv}t + \beta_0^{iv}\right)$$

where

$$\beta_1^{iv} = -\frac{1-\alpha}{\varepsilon}\alpha_1^{iv} \text{ and } \beta_0^{iv} = \alpha_1^{iv} - \frac{1-\alpha}{\varepsilon}\alpha_0^{iv}.$$

It can be checked that

$$-\frac{n}{v} < \dot{y}_4(t) < \frac{3n}{v} \text{ for } t \in I_4 \tag{A-4}$$

where

$$\dot{y}_4(t) = \dot{y}_4^a(t) \text{ for } t \in I_4^a \text{ and } \dot{y}_4(t) = \dot{y}_4^b(t) \text{ for } t \in I_4^b.$$

Interval 5: $I_5 = [t_5, t_6]$ where $t_6 = 6$.

As in interval I_4 , the threshold value $t_{II} = t_I + \theta \approx 5.03$ divides interval I_5 into two subintervals, $I_5^a = [t_5, t_{II}]$ and $I_5^b = [t_{II}, t_6]$. For $t \in I_5^a$, Equation (12) with $\varphi[\dot{y}_4^a(t - \theta)] = v\dot{y}_4^a(t - \theta)$ leads to the solution and its derivative that are the same as the ones obtained in I_4^b ,

$$y_5^a(t) = y_4^b(t) \text{ and } \dot{y}_5^a(t) = \dot{y}_4^b(t) \text{ with } K_5^a = K_4^b.$$

Therefore time trajectories for $t \in I_{II} = I_4^b \cup I_5^a = [t_I, t_{II}]$ are described by

$$y_{II}(t) = y_4^b(t) \text{ and } \dot{y}_{II}(t) = \dot{y}_4^b(t)$$

both of which form (G-II) defined in Section 4.1 where α_j^{iv} and β_j^{iv} for $j = 0, 1$ are written as α_j^{II} and β_j^{II} .

Derivation of (G-III)

Dynamic Equation (12) with $\varphi[\dot{y}_4^b(t - \theta)] = v\dot{y}_4^b(t - \theta)$ for $t \in I_5^b$ has a solution

$$y_5^b(t) = e^{\frac{1-\alpha}{\varepsilon}t} (\alpha_2^v t^2 + \alpha_1^v t + \alpha_0^v)$$

where

$$\begin{aligned} \alpha_2^v &= \frac{v}{\varepsilon} e^{\frac{1-\alpha}{\varepsilon}\theta} \frac{\beta_1^{iv}}{2} \\ \alpha_1^v &= \frac{v}{\varepsilon} e^{\frac{1-\alpha}{\varepsilon}\theta} (\beta_0^{iv} - \theta\beta_1^{iv}) \\ \alpha_0^v &= K_5^b \end{aligned}$$

Solving $y_5^a(t_{II}) = y_5^b(t_{II})$ presents

$$K_5^b \approx 140446.6.$$

Differentiating $y_5^b(t)$ gives

$$\dot{y}_5^b(t) = e^{\frac{1-\alpha}{\varepsilon}t} (\beta_2^v t^2 + \beta_1^v t + \beta_0^v)$$

where

$$\beta_2^v = -\frac{1-\alpha}{\varepsilon} \alpha_2^v, \beta_1^v = 2\alpha_2^v - \frac{1-\alpha}{\varepsilon} \alpha_1^v, \beta_0^v = \alpha_1^v - \frac{1-\alpha}{\varepsilon} \alpha_0^v.$$

Since the $\dot{y}_5^b(t)$ curve crosses the upper horizontal line from below at

$$t_b \approx 5.19395,$$

we then have

$$\begin{aligned} -\frac{n}{v} &< \dot{y}_5^a(t) < \frac{3n}{v} \text{ for } t_5 \leq t \leq t_{II}, \\ -\frac{n}{v} &< \dot{y}_5^b(t) < \frac{3n}{v} \text{ for } t_{II} \leq t \leq t_b, \\ \dot{y}_5^b(t) &> \frac{3n}{v} \text{ for } t_b \leq t \leq t_6. \end{aligned} \tag{A-5}$$

Interval 6: $I_6 = [t_6, t_7]$ where $t_7 = 7$.

Due to the two values, t_{II} and t_b , we define two threshold values $t_{III} = t_{II} + \theta \approx 6.03$ and $t_{IV} = t_b + \theta \approx 6.19$, both of which then divide interval I_6 into three subintervals, $I_6^a = [t_6, t_{III}]$, $I_6^b = [t_{III}, t_{IV}]$ and $I_6^c = [t_{IV}, t_7]$. Accordingly conditions in (A-5) determine the induced investment as

$$\varphi[\dot{y}(t-\theta)] = \begin{cases} \varphi[\dot{y}_5^a(t-\theta)] = v\dot{y}_5^a(t-\theta) & \text{for } t \in I_6^a, \\ \varphi[\dot{y}_5^b(t-\theta)] = v\dot{y}_5^b(t-\theta) & \text{for } t \in I_6^b, \\ \varphi[\dot{y}_5^b(t-\theta)] = 3n & \text{for } t \in I_6^c. \end{cases}$$

In consequence, the form of the solution and its derivative in I_6^a are

$$y_6^a(t) = y_5^b(t) \text{ and } \dot{y}_6^a(t) = \dot{y}_5^b(t).$$

Therefore blue and red trajectories for $t \in I_{III} = I_5^b \cup I_6^a = [t_{II}, t_{III}]$ are described by

$$y_{III}(t) = y_5^b(t) \text{ and } \dot{y}_{III}(t) = \dot{y}_5^b(t)$$

both of which form (G-III) defined in Section 4.1 where α_j^v and β_j^v for $j = 0, 1, 2$ are written as α_j^{III} and β_j^{III} .

Derivation of (G-IV)

For $t \in I_6^b$, successive integral leads to the solution

$$y_6^b(t) = e^{-\frac{1-\alpha}{\varepsilon}t} (\alpha_3^{vi}t^3 + \alpha_2^{vi}t^2 + \alpha_1^{vi}t + \alpha_0^{vi})$$

where

$$\begin{aligned} \alpha_3^{vi} &= \frac{v}{\varepsilon} e^{-\frac{1-\alpha}{\varepsilon}\theta} \frac{\beta_2^v}{2}, \quad \alpha_2^{vi} = \frac{v}{\varepsilon} e^{-\frac{1-\alpha}{\varepsilon}\theta} \frac{\beta_1^v - 2\theta\beta_2^v}{2}, \\ \alpha_1^{vi} &= \beta_0^v - \theta\beta_1^v + \theta^2\beta_2^v, \quad \alpha_0^{vi} = K_6^b. \end{aligned}$$

Solving $y_6^a(t_{III}) = y_6^b(t_{III})$ yields

$$K_6^b \approx -155088.$$

Differentiating $y_6^b(t)$ with respect to t is, after arranging the terms, it can be written as

$$\dot{y}_6^b(t) = e^{-\frac{1-\alpha}{\varepsilon}t} (\beta_3^{vi}t^3 + \beta_2^{vi}t^2 + \beta_1^{vi}t + \beta_0^{vi})$$

where

$$\begin{aligned} \beta_3^{vi} &= -\frac{1-\alpha}{\varepsilon} \alpha_3^{vi}, \\ \beta_2^{vi} &= 3\alpha_3^v - \frac{1-\alpha}{\varepsilon} \alpha_2^{vi}, \\ \beta_1^{vi} &= 2\alpha_2^v - \frac{1-\alpha}{\varepsilon} \alpha_1^{vi}, \\ \beta_0^{vi} &= \alpha_1^v - \frac{1-\alpha}{\varepsilon} \alpha_0^{vi}. \end{aligned}$$

Therefore blue and red trajectories in $I_{IV} = I_6^b$ are described by

$$y_{IV}(t) = y_6^b(t) \text{ and } \dot{y}_{IV}(t) = \dot{y}_6^b(t)$$

both of which form (G-IV) defined in Section 4.1 where α_j^{vi} and β_j^{vi} for $j=0,1,2,3$ are written as α_j^{IV} and β_j^{IV} .

Derivation of (G-V)

For $t \in I_6^c$, Equation (9) implies a form of the solution,

$$y_6^c(t) = e^{\frac{1-\alpha}{\varepsilon}t} K_6^c + \frac{3n}{1-\alpha}$$

$$\dot{y}_6^c(t) = e^{\frac{1-\alpha}{\varepsilon}t} \left(-\frac{1-\alpha}{\varepsilon} K_6^c \right)$$

where solving $y_6^b(t_{IV}) = y_6^c(t_{IV})$ gives

$$K_6^c \approx -2839.05.$$

Interval 7: $I_7 = [t_7, t_8]$ where $t_8 = 8$.

Since Equation (2) implies $\varphi[\dot{y}_6^n(t-\theta)] = 3n$ for $n=a,b,c$ and $t \in I_7$, Equation (9) implies that

$$y_7(t) = y_6^c(t),$$

$$\dot{y}_7(t) = \dot{y}_6^c(t).$$

Notice that the $\dot{y}_7(t)$ curve intersects the horizontal dotted line at $3n/\nu$ from above at the following point,

$$t_c \approx 7.78001.$$

Thereby,

$$\dot{y}_7(t) > \frac{3n}{\nu} \quad \text{for } t_7 \leq t < t_c,$$

$$-\frac{n}{\nu} < \dot{y}_7(t) < \frac{3n}{\nu} \quad \text{for } t_c < t \leq t_8. \tag{A-7}$$

Interval 8: $I_8 = [t_8, t_9]$ where $t_9 = 9$.

The threshold value in interval I_7 defines a new threshold value $t_V = t_c + \theta \approx 8.78$ in interval I_8 that divides interval I_8 into two subintervals, $I_8^a = [t_8, t_V]$ and $I_8^b = [t_V, t_9]$. Since $\varphi[\dot{y}_7(t-\theta)] = 3n$ for $t \in I_8^a$, (9) implies

$$y_8^a(t) = y_7(t) \text{ and } \dot{y}_8^a(t) = \dot{y}_7(t)$$

Therefore trajectories in $I_V = I_6^c \cup I_7 \cup I_8^a = [t_{IV}, t_V]$ are described by

$$y_V(t) = y_6^c(t) = y_7(t) = y_8^a(t) \text{ and } \dot{y}_V(t) = \dot{y}_6^c(t) = \dot{y}_7(t) = \dot{y}_8^a(t).$$

$y_V(t)$ and $\dot{y}_V(t)$ construct (G-V) defined in Section 4.1 where K_6^c is replaced with K_V .

Derivation of (G-VI)

On the other hand, $\varphi[\dot{y}_7(t-\theta)] = \nu \dot{y}_7(t-\theta)$ for $t \in I_8^b$, successive integration implies that the solution of $y(t)$ has the form,

$$y_8^b(t) = e^{\frac{1-\alpha}{\varepsilon}t} (\alpha_1^{viii} t + \alpha_0^{viii})$$

where

$$\alpha_1^{viii} = -\frac{\nu(1-\alpha)}{\varepsilon^2} K_8^b e^{\frac{1-\alpha}{\varepsilon}\theta},$$

$$\alpha_0^{viii} = K_8^b \approx -155088.$$

Time differentiation of $y_8^b(t)$ is

$$\dot{y}_8^b(t) = e^{-\frac{1-\alpha}{\varepsilon}t} (\beta_1^{viii}t + \beta_0^{viii})$$

where

$$\beta_1^{viii} = -\frac{1-\alpha}{\varepsilon}\alpha_1^{viii}, \quad \beta_0^{viii} = \alpha_1^{viii} - \frac{1-\alpha}{\varepsilon}\alpha_0^{viii}.$$

It can be checked that

$$\begin{aligned} -\frac{n}{v} < \dot{y}_8^a(t) < \frac{3n}{v} \quad \text{for } t \in I_8^a \\ -\frac{n}{v} < \dot{y}_8^b(t) < \frac{3n}{v} \quad \text{for } t \in I_8^b. \end{aligned} \tag{A-8}$$

Interval 9: $I_9 = [t_9, t_{10}]$ where $t_{10} = t_9 + \theta$.

The threshold value $t_{VI} = t_V + \theta$ divides interval I_9 into two subintervals, $I_9^a = [t_9, t_{VI}]$ and $I_9^b = [t_{VI}, t_9]$. Since the first equation of (A-8) implies $\varphi[\dot{y}_8(t - \theta)] = v\dot{y}_8^a(t - \theta)$ for $t \in I_9^a$, the solution of (12) is

$$y_9^a(t) = y_8^b(t) \quad \text{and} \quad \dot{y}_9^a(t) = \dot{y}_8^b(t)$$

Therefore trajectories in $I_{VI} = I_8^b \cup I_9^a = [t_V, t_{VI}]$ are described by

$$y_{VI}(t) = y_8^b(t) = y_9^a(t) \quad \text{and} \quad \dot{y}_{VI}(t) = \dot{y}_8^b(t) = \dot{y}_9^a(t)$$

both of which form (G-VI) defined in Section 4.1 where α_j^{viii} and β_j^{viii} for $j = 0, 1$, are written as α_j^{VI} and β_j^{VI} .

Derivation of (G-VII)

On the other hand, $\varphi[\dot{y}_8(t - \theta)] = v\dot{y}_8^b(t - \theta)$ for $t \in I_9^b$ implies the following form of the solution,

$$y_9^b(t) = e^{-\frac{1-\alpha}{\varepsilon}t} (\alpha_2^{ix}t^2 + \alpha_1^{ix}t + \alpha_0^{ix})$$

where

$$\begin{aligned} \alpha_2^{ix} &= \frac{v}{\varepsilon} e^{-\frac{1-\alpha}{\varepsilon}\theta} \frac{\beta_1^{viii}}{2}, \\ \alpha_1^{ix} &= \frac{v}{\varepsilon} e^{-\frac{1-\alpha}{\varepsilon}\theta} (\beta_0^{viii} - \theta\beta_1^{viii}), \\ \alpha_0^{ix} &= K_9^b \approx -7.0415 \times 10^6 \end{aligned}$$

and

$$\dot{y}_9^b(t) = e^{-\frac{1-\alpha}{\varepsilon}t} (\beta_2^{ix}t^2 + \beta_1^{ix}t + \beta_0^{ix})$$

where

$$\begin{aligned} \beta_2^{ix} &= -\frac{1-\alpha}{\varepsilon}\alpha_3^{ix}, \\ \beta_1^{ix} &= 2\alpha_2^{IX} - \frac{1-\alpha}{\varepsilon}\alpha_1^{ix}, \\ \beta_0^{ix} &= \alpha_1^{IX} - \frac{1-\alpha}{\varepsilon}\alpha_0^{ix}. \end{aligned}$$

It is to be noticed that the $\dot{y}_6^a(t)$ curve intersects the horizontal line at $-n/v$ from above at

$$t_d \approx 9.04967$$

with which

$$\dot{y}_9^a(t) > -\frac{n}{v} \text{ for } t_9 \leq t < t_d$$

and

$$(\dot{y}_9^a(t), \dot{y}_9^b(t)) < -\frac{n}{v} \text{ for } t_d < t \leq t_9.$$

Interval 10: $I_{10} = [t_{10}, t_E]$ where $t_E \approx 11.05729$.

The threshold value $t_{VII} = t_d + \theta \approx 10.04$ divides interval I_{10} into two sub-intervals, $I_{10}^a = [t_{10}, t_{VII}]$ and $I_{10}^b = [t_{VII}, t_E]$. Since $\varphi[\dot{y}_9^a(t - \theta)] = v\dot{y}_9^a(t - \theta)$ for $t \in I_{10}^a$, we have

$$y_{10}^a(t) = y_9^b(t) \text{ and } \dot{y}_{10}^a(t) = \dot{y}_9^b(t)$$

Therefore time trajectories in $I_{VII} = I_9^b \cup I_{10}^a = [t_{VI}, t_{VII}]$ are described by

$$y_{VII}(t) = y_9^b(t) = y_{10}^a(t) \text{ and } \dot{y}_{VII}(t) = \dot{y}_9^b(t) = \dot{y}_{10}^a(t)$$

both of which form (G-VII) defined in Section 4.1 where α_j^{ix} and β_j^{ix} for $j = 0, 1$ are written as α_j^{VII} and β_j^{VII} .

Derivation of (G-VIII)

On the other hand $\varphi[\dot{y}_9^a(t - \theta)] = \varphi[\dot{y}_9^b(t - \theta)] = -n$ for $t \in I_{10}^b$ implies that

$$y_{10}^b(t) = e^{-\frac{1-\alpha}{\varepsilon}t} K_{10}^b + \left(-\frac{n}{1-\alpha}\right) \text{ with } K_{10}^b \approx 66133.895$$

and

$$\dot{y}_{10}^b(t) = e^{-\frac{1-\alpha}{\varepsilon}t} \left(-\frac{1-\alpha}{\varepsilon} K_{10}^b\right).$$

The end point \tilde{t}_e is obtained by solving $y_{10}^b(t) = y_1(t_s)$ for t . Therefore time trajectories in $I_{VIII} = I_{10}^b$ are given by

$$y_{VIII}(t) = y_{10}^b(t) \text{ and } \dot{y}_{VIII}(t) = \dot{y}_{10}^b(t)$$

$y_{VIII}(t)$ and $\dot{y}_{VIII}(t)$ form (G-VIII) defined in Section 4.1 where K_{10}^b is denoted by K_{VIII} . A cycle starts at $t = t_s$ $y_1(t_s) \approx 2.02$ and finishes at $t = t_E$ with $y_{VIII}(t_E) \approx 2.02$. The length of this cycle is equal to $t_E - t_s$ that is about 10.06.

Appendix II

Our main aim of this appendix is to analytically reproduce these numerical results of sawtooth oscillations to understand why a trajectory $y(t)$ has kinks (alternatively, its derivative $\dot{y}(t)$ makes jumps). To this end, we start to divide the whole interval $I = [0, 5]$ into five subintervals with respect to the length of

delay $\theta = 1$,

$$I_i = [t_{i-1}, t_i] \text{ for } i = 1, 2, 3, 4, 5$$

with $t_i = i$ and $t_i = t_{i-1} + \theta$.

Derivative of (S-I)

Interval I: $I_1 = [t_0, t_1]$ where $t_0 = 0$ and $t_1 = 1$.

Equation (13) with the constant initial function $y_0(t - \theta) = \Phi(t - \theta)$ yields the solution of the form

$$y_1(t) = e^{\frac{1-\alpha}{\varepsilon}t} \cdot K_1 \text{ with } K_1 = -2$$

and differentiation gives its derivative form

$$\dot{y}_1(t) = e^{\frac{1-\alpha}{\varepsilon}t} \cdot \left(-\frac{1-\alpha}{\varepsilon} K_1 \right).$$

Both of which form (S-I) defined in Section 5.1. Since $\dot{y}_1(t_0) = 1.6$, $\dot{y}_1(t_1) \approx 0.719$ and $\dot{y}_1(t) > 0$ for $t \in I_1$, $\dot{y}_1(t)$ stays in the middle region,

$$-\frac{n}{k} \leq \dot{y}_1(t) \leq \frac{3n}{k} \text{ for } t \in I_1. \tag{A-9}$$

Derivative of (S-II)

Interval II: $I_2 = [t_1, t_2]$ where $t_2 = t_1 + \theta$.

Due to (2) and (A-9),

$$\varphi[\dot{y}_1(t - \theta)] = v \cdot \dot{y}_1(t - \theta)$$

which is substituted into (13) to obtain,

$$\dot{y}(t) + \frac{1-\alpha}{\varepsilon} y(t) = Q(t) \text{ with } Q(t) = -\frac{k(1-\alpha)}{\varepsilon^2} K_1 e^{\frac{1-\alpha}{\varepsilon}\theta} e^{\frac{1-\alpha}{\varepsilon}t}.$$

Since this equation can be written as

$$\frac{d}{dt} \left(y(t) e^{\frac{1-\alpha}{\varepsilon}t} \right) = Q(t) e^{\frac{1-\alpha}{\varepsilon}t}$$

Integrating both sides and arranging the terms present the solution of $y(t)$, denoted as $y_2(t)$,

$$y_2(t) = e^{\frac{1-\alpha}{\varepsilon}t} \left[\left(-\frac{k(1-\alpha)}{\varepsilon^2} K_1 e^{\frac{1-\alpha}{\varepsilon}\theta} \right) t + K_2 \right].$$

Since the trajectory of $y_2(t)$ is piecewise continuous, solving $y_1(t_1) = y_2(t_1)$ presents

$$K_2 \approx -16.244.$$

The form of $y_2(t)$ is rewritten as

$$y_2(t) = e^{\frac{1-\alpha}{\varepsilon}t} (\alpha_1'' t + \alpha_0'')$$

with

$$\alpha_1'' = -\frac{k(1-\alpha)}{\varepsilon^2} K_1 e^{\frac{1-\alpha}{\varepsilon} t} \approx 14.244 \text{ and } \alpha_0'' = K_2$$

A time derivative of $y_2(t)$ is

$$\dot{y}_2(t) = e^{\frac{1-\alpha}{\varepsilon} t} (\beta_1'' t + \beta_0'')$$

with

$$\beta_1'' = -\frac{k(1-\alpha)^2}{\varepsilon^3} e^{\frac{1-\alpha}{\varepsilon} t} K_1 \approx -11.395$$

$$\text{and } \beta_0'' = -\frac{1-\alpha}{\varepsilon} \left(\frac{k}{\varepsilon} e^{\frac{1-\alpha}{\varepsilon} t} K_1 + K_2 \right) \approx 27.238.$$

These $y_2(t)$ and $\dot{y}_2(t)$ form (S-II) defined in Section 5.1. Under Assumption 1, we calculate the boundary values of interval I_2 ,

$$y_2(t_1) \approx -0.899, \dot{y}_2(t_1) \approx 7.119 \text{ and } y_2(t_2) = 2.472 \text{ and } \dot{y}_2(t_2) \approx 0.898.$$

The red curve crosses the upper horizontal dotted line once from above at point

$$t_a = 1.286$$

with which the following inequalities hold, as is seen in I_2 in **Figure 2**,

$$\begin{aligned} \dot{y}_2(t) &> \frac{3n}{v} \text{ for } t_1 \leq t < t_a \\ -\frac{n}{v} < \dot{y}_2(t) < \frac{3n}{v} \text{ for } t_a < t \leq t_2. \end{aligned} \tag{A-10}$$

Derivations of (G-IIIa), (G-IIIb) and (G-IIIc)

Interval III: $I_3 = [t_2, t_3]$ where $t_3 = t_2 + \theta$.

Due to the value of t_a , the interval I_3 is divided into two subintervals, $I_3^a = [t_2^\theta, t_a]$ and $I_3^b = (t_a, t_3]$ where $t_a^\theta = t_a + \theta$. Delay investment is differently determined according to conditions in (A-10),

$$\varphi[\dot{y}_2(t-\theta)] = \begin{cases} 3n & \text{if } t \in I_3^a \\ k\dot{y}_2(t-\theta) & \text{if } t \in I_3^b. \end{cases} \tag{18}$$

different dynamic systems are defined on different subintervals. So we derive the solution of the differential equation in each subinterval.

Interval III-1: $t_2 \leq t < t_a^\theta$.

In this subinterval, Equation (8) with the first equation of (A-11) yields the solution

$$y_3(t) = e^{\frac{1-\alpha}{\varepsilon} t} K_3 + \frac{3n}{1-\alpha}$$

and its derivative

$$\dot{y}_3(t) = -\frac{1-\alpha}{\varepsilon} K_3 e^{\frac{1-\alpha}{\varepsilon} t}$$

where solving $y_3(t_2) = y_2(t_2)$ gives

$$K_3 \approx -99.2.$$

These two functions form (S-IIIa) where $y_3(t)$ and $\dot{y}_3(t)$ are denoted by $y_3^a(t)$ and $\dot{y}_3^a(t)$. Boundary values of this interval are

$$y_3^a(t_2) \approx 2.472, \dot{y}_3^a(t_2) \approx 16.02 \text{ and } y_3^a(t_a^\theta) \approx 6.565, \dot{y}_3^a(t_a^\theta) \approx 12.748.$$

Interval III-2: $t_a^\theta < t \leq t_3$.

In this interval, we have Equation (13) with the second equation of (A-11) that is rewritten as

$$\dot{y}(t) + \frac{1-\alpha}{\varepsilon} y(t) = Q(t)$$

where

$$Q(t) = \frac{k}{\varepsilon} \dot{y}_2(t-\theta) = \frac{k}{\varepsilon^2} e^{-\frac{1-\alpha}{\varepsilon}(t-\theta)} \{ \beta_1''(t-\theta) + \beta_0'' \}.$$

Rewriting the dynamic equation as

$$\frac{d}{dt} \left(y(t) e^{\frac{1-\alpha}{\varepsilon} t} \right) = Q(t) e^{\frac{1-\alpha}{\varepsilon} t}$$

and integrating both sides give the following form of a solution,

$$y_4(t) = e^{-\frac{1-\alpha}{\varepsilon} t} \left\{ \frac{k}{\varepsilon} e^{\frac{1-\alpha}{\varepsilon} \theta} \left[\frac{\beta_1''}{2} t^2 + (\beta_0'' - \theta \beta_1'') t \right] + K_4 \right\}$$

where solving $y_3(t_a^\theta) = y_4(t_a^\theta)$ gives

$$K_4 \approx -480.253.$$

Then the form of $y_4(t)$ is rewritten as

$$y_4(t) = e^{-\frac{1-\alpha}{\varepsilon} t} (\alpha_2''' t^2 + \alpha_1''' t + \alpha_0''')$$

where

$$\alpha_2''' = \frac{k}{\varepsilon} e^{-\frac{1-\alpha}{\varepsilon} \theta} \frac{\beta_1''}{2} \approx -50.719$$

$$\alpha_1''' = \frac{k}{\varepsilon} e^{-\frac{1-\alpha}{\varepsilon} \theta} (\beta_0'' - \theta \beta_1'') \approx 343.918,$$

and

$$\alpha_0''' = K_4.$$

A derivative of $y_4(t)$ is

$$\dot{y}_4(t) = e^{-\frac{1-\alpha}{\varepsilon} t} (\beta_2''' t^2 + \beta_1''' t + \beta_0''')$$

where

$$\beta_2''' = -\frac{1-\alpha}{\varepsilon} \alpha_2''' \approx -22.79,$$

$$\beta_1''' = 2\alpha_2''' - \frac{1-\alpha}{\varepsilon}\alpha_1''' \approx -255.97$$

and

$$\beta_0''' = \alpha_1''' - \frac{1-\alpha}{\varepsilon}\alpha_0''' \approx 559.71.$$

Boundary values are

$$y_4(t_a^\theta) \approx 6.565, \dot{y}_4(t_a^\theta) \approx 12.748$$

and

$$y_4(t_3) \approx 8.621, \dot{y}_4(t_3) \approx -3.309.$$

These $y_4(t)$ and $\dot{y}_4(t)$ form (S-IIIb) in which $y_4(t)$ and $\dot{y}_4(t)$ are denoted as $y_3^b(t)$ and $\dot{y}_3^b(t)$. As is seen in **Figure 6**, the red curve crosses the horizontal dotted lines at $3n/k$ and $-n/k$ once at points

$$t_b \approx 2.535 \text{ with } \dot{y}_3^b(t_b) = \frac{3n}{k}$$

$$t_c \approx 2.843 \text{ with } \dot{y}_3^b(t_c) = -\frac{n}{k}.$$

It is apparent from **Figure 6** that

$$\begin{aligned} \dot{y}_3^a(t) &> \frac{3n}{k} \text{ for } t_3 \leq t < t_a^\theta, \\ \dot{y}_3^b(t) &> \frac{3n}{k} \text{ for } t_{a\theta} \leq t < t_b, \\ \frac{3n}{k} &> \dot{y}_3^b(t) > -\frac{n}{k} \text{ for } t_b < t < t_c, \\ -\frac{n}{k} &> \dot{y}_3^c(t) \text{ for } t_c < t \leq t_3. \end{aligned} \tag{A-12}$$

Derivation of (S-IVa), (S-IVb) and (S-IVc)

Interval IV: $I_4 = [t_3, t_4]$ where $t_4 = t_3 + \theta$.

Due to the properties described in (A-12), interval I_4 is divided into three subintervals by $t_b^\theta = t_b + \theta$ and $t_c^\theta = t_c + \theta$ in which

$$\varphi[\dot{y}_3^a(t-\theta)] = \varphi[\dot{y}_3^b(t-\theta)] = 3n \text{ for } t_3 \leq t < t_b^\theta \tag{A-13}$$

$$\varphi[\dot{y}_3^b(t-\theta)] = k\dot{y}_3^b(t-\theta) \text{ for } t_b^\theta < t < t_c^\theta \tag{A-14}$$

and

$$\varphi[\dot{y}_3^c(t-\theta)] = -n \text{ for } t_c^\theta < t \leq t_4. \tag{A-15}$$

Interval IV-1: $t_3 \leq t < t_b^\theta$

Equation (2) with (A-13) implies that the solution of the differential equation

$$\varepsilon \dot{y}(t) + (1-\alpha)y(t) = 3n$$

is given by

$$y_5(t) = e^{-\frac{1-\alpha}{\varepsilon}t} K_5 + \frac{3n}{1-\alpha} \text{ with } K_5 \approx -152.994$$

where K_5 solves

$$y_4(t_3) = y_5(t_3).$$

A derivative of $y_5(t)$ is

$$\dot{y}_5(t) = e^{-\frac{1-\alpha}{\varepsilon}t} \left(-\frac{1-\alpha}{\varepsilon} K_5 \right) \text{ with } -\frac{1-\alpha}{\varepsilon} K_5 \approx 122.395.$$

These $y_5(t)$ and $\dot{y}_5(t)$ form (S-IVa) in which $y_5(t)$ and $\dot{y}_5(t)$ are denoted as $y_4^a(t)$ and $\dot{y}_4^a(t)$. We then have the boundary values of $y_4^a(t)$ of interval $[t_3, t_b^\theta]$,

$$y_4^a(t_3) \approx 8.621, \dot{y}_4^a(t_3) \approx 11.103 \text{ and } y_4^a(t_b^\theta) \approx 13.456, \dot{y}_4^a(t_b^\theta) \approx 7.236.$$

Interval IV-2: $t_b^\theta < t < t_c^\theta$.

Rewriting the delay differential Equation (2) with (A-14) as

$$\dot{y}(t) + \frac{1-\alpha}{\varepsilon} y(t) = Q(t)$$

where

$$Q(t) = \frac{k}{\varepsilon} \dot{y}_4(t-\theta) = \frac{k}{\varepsilon} e^{-\frac{1-\alpha}{\varepsilon}(t-\theta)} \left\{ \beta_2^{III} (t-\theta)^2 + \beta_1^{III} (t-\theta) + \beta_0^{III} \right\}.$$

Successive integration yields the solution,

$$y_6(t) = e^{-\frac{1-\alpha}{\varepsilon}t} \left\{ \int \frac{k}{\varepsilon} e^{-\frac{1-\alpha}{\varepsilon}\theta} \left[\beta_2^{III} t^2 + (\beta_1^{III} - 2\theta\beta_2^{III})t + (\beta_0^{III} - \theta\beta_1^{III} + \theta^2\beta_2^{III}) \right] dt + K_6 \right\}$$

or

$$y_6(t) = e^{-\frac{1-\alpha}{\varepsilon}t} \left\{ \alpha_3^{IV} t^3 + \alpha_2^{IV} t^2 + \alpha_1^{IV} t + \alpha_0^{IV} \right\}$$

with

$$\begin{aligned} \alpha_3^{IV} &= \frac{k}{\varepsilon} e^{-\frac{1-\alpha}{\varepsilon}\theta} \frac{\beta_2^{III}}{3} \approx 180.604, \\ \alpha_2^{IV} &= \frac{k}{\varepsilon} e^{-\frac{1-\alpha}{\varepsilon}\theta} \frac{\beta_1^{III} - 2\theta\beta_2^{III}}{2} \approx -2037.36, \\ \alpha_1^{IV} &= \frac{k}{\varepsilon} e^{-\frac{1-\alpha}{\varepsilon}\theta} (\beta_0^{III} - \theta\beta_1^{III} + \theta^2\beta_2^{III}) \approx 10195.4, \\ \alpha_0^{IV} &= K_6 \approx -15672.428 \end{aligned}$$

where K_6 solves

$$f_5(t_b^\theta) = f_6(t_b^\theta).$$

A derivative of $y_6(t)$ is

$$\dot{y}_6(t) = e^{-\frac{1-\alpha}{\varepsilon}t} \left\{ \beta_3^{IV} t^3 + \beta_2^{IV} t^2 + \beta_1^{IV} t + \beta_0^{IV} \right\}$$

with

$$\begin{aligned}\beta_3^{IV} &= -\frac{1-\alpha}{\varepsilon}\alpha_3^{IV} \approx -96.322, \\ \beta_2^{IV} &= 3\alpha_3^{IV} - \frac{1-\alpha}{\varepsilon}\alpha_2^{IV} \approx 1991.1, \\ \beta_1^{IV} &= 2\alpha_2^{IV} - \frac{1-\alpha}{\varepsilon}\alpha_1^{IV} \approx -12231, \\ \beta_0^{IV} &= \alpha_1^{IV} - \frac{1-\alpha}{\varepsilon}\alpha_0^{IV} \approx 22733.3\end{aligned}$$

These $y_6(t)$ and $\dot{y}_6(t)$ form (S-IVb) in which $y_6(t)$ and $\dot{y}_6(t)$ are denoted as $y_4^b(t)$ and $\dot{y}_4^b(t)$. The boundary values of the interval are

$$y_4^b(t_b^\theta) \approx 13.455, \dot{y}_4^b(t_b^\theta) \approx 7.236 \text{ and } y_4^b(t_c^\theta) \approx 11.677, \dot{y}_4^b(t_c^\theta) \approx -15.342.$$

Further the downward-sloping curve of $\dot{y}_4^b(t)$ intersects each of the two dotted horizontal lines at $3n/k$ and $-n/k$ at the points

$$t_d \approx 3.561 \text{ with } \dot{y}_4^b(t_d) = \frac{3n}{k}$$

and

$$t_e \approx 3.624 \text{ with } \dot{y}_4^b(t_e) = -\frac{n}{k}.$$

Interval IV-3: $t_c^\theta < t \leq t_4$

Equation (A-15) implies that the dynamic Equation (2) has the following forms for the solution $y_7(t)$ and its derivative $\dot{y}_7(t)$

$$y_7(t) = e^{\frac{1-\alpha}{\varepsilon}t} K_7 - \frac{n}{1-\alpha} \text{ with } K_7 \approx 415.092$$

an

$$\dot{y}_7(t) = e^{\frac{1-\alpha}{\varepsilon}t} \left(-\frac{1-\alpha}{\varepsilon} K_7 \right) \text{ with } -\frac{1-\alpha}{\varepsilon} K_7 \approx -340.074$$

where K_7 solves

$$y_6(t_c^\theta) = y_7(t_c^\theta).$$

These $y_7(t)$ and $\dot{y}_7(t)$ form (S-IVc) in which $y_7(t)$ and $\dot{y}_7(t)$ are denoted as $y_4^c(t)$ and $\dot{y}_4^c(t)$. The boundary values of the interval are

$$y_4^c(t_c^\theta) \approx 11.671, \dot{y}_4^c(t_c^\theta) \approx -15.342 \text{ and } y_4^c(t_4) \approx 9.420, \dot{y}_4^c(t_4) \approx -13.536$$

It is seen that

$$\begin{aligned}\dot{y}_4^a(t) &> \frac{3n}{k} \text{ for } t_3 \leq t < t_b^\theta, \\ \dot{y}_4^b(t) &> \frac{3n}{k} \text{ for } t_b^\theta \leq t < t_d, \\ \frac{3n}{k} &> \dot{y}_4^b(t) > -\frac{n}{k} \text{ for } t_d < t < t_e, \\ -\frac{n}{k} &> \dot{y}_4^b(t) \text{ for } t_e < t \leq t_4.\end{aligned}$$

Derivation of (S-V)

Interval V: $I_5 = [t_4, t_5]$

Due to the threshold values, t_A^{IV} and t_B^{IV} , interval I_5 is divided into three subintervals by $t_A^V = t_A^{IV} + \theta$ and $t_B^V = t_B^{IV} + \theta$ in which

$$\varphi[\dot{f}_5(t - \theta)] = \varphi[\dot{f}_6(t - \theta)] = 3n \text{ for } t_4 \leq t < t_A^V \tag{A-16}$$

$$\varphi[\dot{f}_6(t - \theta)] = k\dot{f}_6(t - \theta) \text{ for } t_A^V < t < t_B^V \tag{A-17}$$

and

$$\varphi[\dot{f}_7(t - \theta)] = -n \text{ for } t_B^V < t \leq t_5. \tag{A-18}$$

Repeating the same procedure done just above, we can derive the explicit forms of a solution of the delay dynamic equation.

Interval V-1: $t_4 \leq t < t_A^V$.

Equation (8) with (A-16) presents the following forms of the solutions,

$$f_8(t) = e^{\frac{1-\alpha}{\varepsilon}t} K_8 + \frac{3n}{1-\alpha} \text{ with } K_8 \approx -320.88$$

and

$$\dot{f}_8(t) = e^{\frac{1-\alpha}{\varepsilon}t} \left(-\frac{1-\alpha}{\varepsilon} K_8 \right) \text{ with } -\frac{1-\alpha}{\varepsilon} K_8 \approx 256.704$$

where K_8 solves $f_7(t_4) = f_8(t_4)$. These $f_8(t)$ and $\dot{f}_8(t)$ form (S-Va) in which $f_8(t)$ and $\dot{f}_8(t)$ are replaced with $y_5^a(t)$ and $\dot{y}_5^a(t)$.

Interval V-2: $t_A^V < t < t_B^V$.

Applying successive integration to Equation (2) with (A-17) yields the following forms of the solutions,

$$f_9(t) = e^{\frac{1-\alpha}{\varepsilon}t} \{ \alpha_4^V t^4 + \alpha_3^V t^3 + \alpha_2^V t^2 + \alpha_1^V t + \alpha_0^V \}$$

with

$$\alpha_4^V = \frac{k}{\varepsilon} e^{\frac{1-\alpha}{\varepsilon}\theta} \frac{\beta_3^{IV}}{3} \approx -214.369$$

$$\alpha_3^V = \frac{k}{\varepsilon} e^{\frac{1-\alpha}{\varepsilon}\theta} \frac{\beta_2^{IV} - 3\theta\beta_3^{IV}}{3} \approx 6765.83,$$

$$\alpha_2^V = \frac{k}{\varepsilon} e^{\frac{1-\alpha}{\varepsilon}\theta} \frac{\beta_1^{IV} - 2\theta\beta_2^{IV} + 3\theta^2\beta_3^{IV}}{2} \approx -73452.5,$$

$$\alpha_1^V = \frac{k}{\varepsilon} e^{\frac{1-\alpha}{\varepsilon}\theta} (\beta_0^{IV} - \theta\beta_1^{IV} + \theta^2\beta_2^{IV} - \theta^3\beta_3^{IV}) \approx 329841,$$

$$\alpha_0^V = K_9 \approx -525029$$

where K_9 solves $f_8(t_A^V) = f_9(t_A^V)$. A derivative of $f_6(t)$ is

$$\dot{f}_9(t) = e^{\frac{1-\alpha}{\varepsilon}t} \{ \beta_4^V t^4 + \beta_3^V t^3 + \beta_2^V t^2 + \beta_1^V t + \beta_0^V \}$$

with

$$\begin{aligned}\beta_4^V &= -\frac{1-\alpha}{\varepsilon}\alpha_4^{IV} \approx 171.495, \\ \beta_3^V &= 4\alpha_4^V - \frac{1-\alpha}{\varepsilon}\alpha_3^V \approx -9270.135, \\ \beta_2^V &= 3\alpha_3^V - \frac{1-\alpha}{\varepsilon}\alpha_2^V \approx 79059.451, \\ \beta_1^V &= 2\alpha_2^V - \frac{1-\alpha}{\varepsilon}\alpha_1^V \approx -410777.286, \\ \beta_0^V &= \alpha_1^V - \frac{1-\alpha}{\varepsilon}\alpha_0^V \approx 749863.287\end{aligned}$$

These $f_9(t)$ and $\dot{f}_9(t)$ form (S-Vb) in which $f_9(t)$ and $\dot{f}_9(t)$ are replaced with $y_5^b(t)$ and $\dot{y}_5^b(t)$. As is seen in **Figure 6**, the red curve crosses the horizontal dotted lines at $3n/k$ and $-n/k$ once at points

$$\begin{aligned}t_f &\approx 4.566 \text{ with } \dot{y}_5^b(t_f) = \frac{3n}{k} \\ t_g &\approx 4.581 \text{ with } \dot{y}_5^b(t_g) = -\frac{n}{k}.\end{aligned}$$

To avoid notational congestion in **Figure 6**, t_f and t_g are not labelled.

Interval IV-3: $t_B^V < t \leq t_5$

Equation (8) with (A-18) presents the following forms of the solutions,

$$f_{10}(t) = e^{\frac{1-\alpha}{\varepsilon}t} K_{10} - \frac{n}{1-\alpha} \text{ with } K_{10} \approx 860.508$$

and

$$\dot{f}_{10}(t) = e^{\frac{1-\alpha}{\varepsilon}t} \left(-\frac{1-\alpha}{\varepsilon} K_{10} \right) \text{ with } -\frac{1-\alpha}{\varepsilon} K_{10} \approx -688.406$$

where K_{10} solves $f_9(t_B^V) = f_{10}(t_B^V)$. These $f_{10}(t)$ and $\dot{f}_{10}(t)$ form (S-Vc) in which $f_{10}(t)$ and $\dot{f}_{10}(t)$ are replaced with $y_5^c(t)$ and $\dot{y}_5^c(t)$.

It is seen that

$$\begin{aligned}\dot{y}_5^a(t) &> \frac{3n}{k} \text{ for } t_4 \leq t < t_d^\theta, \\ \dot{y}_5^b(t) &> \frac{3n}{k} \text{ for } t_d^\theta \leq t < t_f, \\ \frac{3n}{k} &> \dot{y}_5^b(t) > -\frac{n}{k} \text{ for } t_f < t < t_g, \\ -\frac{n}{k} &> \dot{y}_5^c(t) \text{ for } t_g < t \leq t_5.\end{aligned}$$